QUASI-HARMONIC FRICTION INDUCED VIBRATION

by

PAK LIM KO

Associate of the Royal College of Science & Technology,
Glasgow, 1963.

A THESIS SUBMITTED IN PARTIAL FULFILMENT OF
THE REQUIREMENTS FOR THE DEGREE OF

MASTER OF APPLIED SCIENCE

in the Department

of

Mechanical Engineering

We accept this thesis as conforming to the
required standard

THE UNIVERSITY OF BRITISH COLUMBIA

APRIL, 1965

In presenting this thesis in partial fulfilment of the requirements for an advanced degree at the University of British Columbia, I agree that the Library shall make it freely available for reference and study. I further agree that permission for extensive copying of this thesis for scholarly purposes may be granted by the Head of my Department or by his representatives. It is understood that copying or publication of this thesis for financial gain shall not be allowed without my written permission.

Department of **Mechanical Engineering**

The University of British Columbia,
Vancouver 8, Canada.

Date **April 28, 1965**

ABSTRACT

The behaviour of the quasi-harmonic type frictional oscillation for steel sliding surfaces was investigated both experimentally and theoretically.

The kinetic coefficient of friction, which was expressed as a function of sliding velocity, was represented by a polynomial. The slowly varying amplitude and phase method of Kryloff and Bogoliuboff was used to solve the non-linear differential equation of motion. The calculations were carried out on the computer. The theoretical analysis suggests that the amplitude of the quasi-harmonic oscillation increases almost linearly as the driven surface velocity increases until a critical velocity is reached where the friction-velocity curve begins to flatten out. Beyond this point the oscillation diminishes to zero.

Experiments were carried out mainly on unlubricated surfaces at driven surface velocities ranging from 0.5 in/sec to 25 in/sec. The results revealed that for short running distances frictional oscillation of the stick-slip type could occur. Frictional oscillation of the quasi-harmonic type existed in the system when negative slope appeared in the low velocity region of the friction-velocity curve after a run-in period. The growth and decay of the vibration amplitude with variation in driven surface velocity has been observed and this substantiates the findings of the theoretical analysis.

ACKNOWLEDGEMENT

The author wishes to express his thanks to Professor W.O. Richmond for the use of the facilities of the Department of Mechanical Engineering, to the Staff of the Mechanical Engineering Laboratory and the Lubrication Laboratory for their valuable assistance, to the faculty and graduate students in the Department of Mechanical Engineering for their many helpful suggestions.

Special thanks are due to his research supervisor, Dr. C.A. Brockley, for his guidance and constant encouragement.

The experimental work of this thesis was carried out in the Lubrication Laboratory, Department of Mechanical Engineering and the theoretical data was compiled in the Computing centre, University of British Columbia. The use of these special facilities is gratefully acknowledged. Financial Assistance was received from the Defence Research Board of Canada under Grant number 7510-31.

NOMENCLATURE

Symbol		Units
k	Stiffness of the slider suspension	lb/in
r	Damping coefficient of the slider suspension	lb sec/in
W	Normal force on slider	lb
M	Equivalent mass of the vibrating parts	lb sec^2/in
X	Displacement of the slider	in.
$\dot{X}$	Velocity of the slider	in/sec
$\ddot{X}$	Acceleration of the slider	in/sec^2
v	Driven surface velocity	in/sec
F_f	Friction force	lb.
t	Time	sec
α	Amplitude of stick-slip vibration	in.
μ_S	Static coefficient of friction	
μ_K	Kinetic coefficient of friction	
μ_L	Lower limit of static frictional coefficient	
μ_u	Upper limit of static frictional coefficient	
ω	Natural frequency of the vibrating system	rad/sec
ω_d	Damped natural frequency of the vibrating system	rad/sec
λ	Damping parameter - Stick-slip	
A	Amplitude of quasi-harmonic oscillation	in.
Φ	Phase angle	
β	Angular displacement of slider	rad.
S	Slope of the linear section of the friction-velocity curve - stick-slip	

TABLE OF CONTENTS

LIST OF FIGURES

List of Figures cont.

CHAPTER I

1. Introduction

Vibrations produced by friction are sometimes referred to as mechanical relaxation oscillations or self-excited oscillations. In general, self-excited oscillations are steady oscillations sustained by forces created by the motion itself and disappear when the motion stops. The shape of the oscillation may be either of the saw tooth type (stick-slip) or nearly sinusoidal in form.

Self-excited frictional oscillations occur in a variety of systems. Some forms of the oscillation are used for sound production but in the engineering fields self-excited phenomena are usually unwanted. Tool chatter, brake squeaking, jerky motion of rubbing elements in instruments, are examples of undesirable mechanical relaxation oscillations. They can be detrimental to accurate positioning in servomechanisms operating at creep speeds or may lead to surface damage and failure of machine components. Thus the problems arising from vibratory sliding motions are so frequently encountered and often of such severity, that the application of preventative measures becomes imperative and a full understanding of the nature of the mechanisms is important.

Many workers in this field have considered the problem and discussed it from different points of view; in particular, stick-slip phenomena have been widely considered. The present investigation is concerned with the near-sinusoidal form of frictional oscillations which are observed mainly at higher sliding speeds.

2. Historical Background

Many writers have noted that if a frictional force versus velocity curve has a negative slope, self-excited oscillations can result. One of the earliest experiments with self-excited mechanical oscillations was made by W. Froude [1]. His experiments were concerned with a pendulum swinging from a shaft; he found that vibrations of the pendulum might be maintained or even increased by rotation of the shaft.

Thomas [2] studied the dynamics of the self-excited type of oscillations both graphically and analytically. He showed that in the absence of viscous damping, stable oscillations of the simple harmonic type could occur under conditions where the coefficient of kinetic friction is equal to the coefficient of static friction, with the coefficient of kinetic friction being independent of the sliding velocity. However, stable oscillations of the stick-slip type could occur if the coefficient of kinetic friction is smaller than the coefficient of static friction. He also showed that the simple harmonic type oscillations can no longer be sustained in the presence of viscous damping but if the damping is not excessive the stick-slip type oscillations can be maintained.

In his investigation of the mechanics of the skidding of automobile tires, Papenhuyzen [3] has revealed some fundamental aspects of frictional oscillations. He showed that at low driven surface velocities the vibrating member remained stationary at a constant displaced position. As the driven surface velocity increased to a distinctly defined first critical value the relaxation oscillations of the so called stick-slip type appeared. The speed of micro-slip during the sticking stage increased with increasing driven surface velocity until the driven surface velocity reached a second critical value, where the speed of slipping was equal to the first critical driven surface velocity. At surface velocities above the second critical value frictional oscillations of the simple harmonic type occurred.

Bowden and Leben [4] carried out a series of experiments on the friction between sliding metals in the absence of a lubricating film. In most cases their experiments demonstrated frictional oscillations of the stick-slip type. In their experiments the recorded sliding velocities were very high in comparison with the driven surface velocity. They indicated that there were high temperature flashes during the slip stage of the stick-slip type oscillations. Thus they suggested that local welding could result from the high temperature. However, Blok [5] indicated that it is unlikely that welding effects are the main reason for the occurrence of the frictional oscillations. He suggested that the essential condition for the occurrence of frictional oscillations is decreasing frictional force at increasing sliding velocity. He showed and discussed three possible types of friction-velocity curve and analysed a linearised case in detail. In his analysis, he determined a limiting condition for the relaxation oscillation to exist by means of a relationship plotted between dimensionless parameters of damping and sliding velocity.

Further investigation of the temperature flash during the stick-slip process was carried out by Morgan, Muskat and Reed [6]. In 1943, these authors together with Sampson [7], studied the friction behaviour during the slip portion of the stick-slip process. They showed that the friction-velocity relation is not reversible. They also indicated that there is evidence that the friction does not return immediately to its higher static value when the two surfaces come to rest.

Rabinowicz [8] explained the higher static coefficient as being due to the metallic junctions becoming stronger after the surfaces have been in stationary contact for some time. He also developed an experimental method to show that the static coefficient persists for transverse displacements of the order of 10^{-4} cm and then falls off gradually to the kinetic coefficient.

Various kinds of sliding surfaces and lubricants were used by Bristow [9], [10] to study the friction-velocity relationship. Temperature effects were also studied. He confirmed that the existence of a negative friction-velocity relationship is a necessary condition for relaxation oscillations to be excited in an elastic system. He also indicated that the total movement of the elastic system during the stick stage was less than the movement of the lower surface in the same time and this movement of the elastic system decreases as the velocity of the moving surface increases, eventually the velocity of the movement during stick equals the speed of moving surface and relaxation oscillations cease. At still greater speeds quasi-sinusoidal oscillations may occur.

A simple graphical method for determining the vibration cycle from any friction-velocity curve was developed by Dudley and Swift [11]. The method makes direct use of the experimental friction-velocity curve. A number of representative cases where the frictional coefficient varies with relative sliding velocity were investigated. They showed that stick-slip oscillations will develop and persist under certain frictional and velocity conditions while under others oscillation will decay. They also pointed out that in some cases either stick-slip oscillation or decay can occur according to initial displacement. They concluded that slow driven surface velocities lead to stick-slip oscillations and the amplitude of these oscillations increases as the speed increases, and at a certain critical velocity the oscillations die out. At an intermediate velocity between stick-slip and decay and under certain combinations of frictional characteristic and damping, quasi-sinusoidal oscillations may occur.

In his investigation of automobile brake squeal, Sinclair [12] once again confirmed that frictional vibrations are caused by an inverse variation of coefficient of friction with sliding velocity. He also suggested that decrease in friction observed at high sliding velocity is caused by high temperatures developed at high velocity. This behaviour was further explained by Rabinowicz [13]. He indicated that the negative friction-velocity shape at high velocity is connected with thermal softening which produces a low shear surface film on a harder substratum. He defined the regular stick-slip oscillations as being time controlled and the quasi-sinusoidal oscillations as being velocity controlled.

Derjaguin, Push and Tolstoi [14] presented a very detailed theoretical analysis of the relaxation oscillations. In their analysis the friction-velocity curve was assumed to be linear and in the later part of the analysis a condition was established to make the theory valid for a time dependent static frictional coefficient. They defined conditions for the disappearance of the stick-slip oscillations and established equations for determining the critical driven surface velocity at this point. The method does not give accurate predictions. Singh [15] used the general method of analysis employed by Derjaguin, et al, in an experimental study of critical velocity.

Cook [16] made a theoretical analysis of the dynamic friction between two sliding surfaces. Frictional characteristic in the high speed region as well as for lubricated surfaces were considered but insufficient experimental results were available to support the theory.

Potter [17] and Cameron [18] both studied the frictional oscillations at low driven surface velocities. Potter's apparatus had a very limited range of driven surface velocities thus preventing a thorough investigation of the critical conditions for the disappearance of stick-slip oscillations. A different driving mechanism for the driven surface was used in Cameron's apparatus which gave him a much wider range of surface velocity. A very detailed theoretical analysis was developed for the stick-slip process based on the assumption that the kinetic frictional coefficient varied linearly with the sliding velocity and that there was instant drop from static friction to kinetic friction. An equation for the amplitude of oscillations was developed by combining the graphical and theoretical methods. More recently Brockley, Cameron and Potter [19] presented a summary of the results on the behaviour of the stick-slip type frictional oscillations.

In 1963, Jarvis and Mills [20] developed a mathematical theory for the oscillation of a special system. The system they investigated consisted of two continuous elastic bodies coupled by sliding friction, as in a vehicle brake. Their investigation shows that unwanted vibration in any system can possibly be avoided by careful choice of dimensions in the design. The significance of their work is the demonstration of the 'geometrically induced' instability of two elastic components interacting through the agency of kinetic dry friction which is a phenomenon distinct from the vibration induced by kinetic friction with negative characteristic.

Kosterin and Kraghelsky [21] studied the frictional oscillations in connection with an automobile clutch system. The frictional force in the equation of motion was expressed as a function of the vibrational velocity and an exponential term was included in the expression but no further analysis was carried out, instead, the Lienard's graphical construction was used to investigate the friction-velocity characteristic. In 1961, the same authors [22] related the time dependent dry friction with the stress and strain in the contacting surfaces and derived an equation describing friction as a function of material properties and time. They showed that the rheological properties of the contacting materials would influence the friction force.

In all the previous work on self-excited oscillations due to negative damping very little consideration has been given to the quasi-sinusoidal oscillations which occur at high sliding velocities. In most of the theoretical analyses the friction-velocity curves are linearised, which is true only under certain conditions. Amplitude - velocity relationships in the high speed region have received very little attention.

The present work relates to a theoretical and experimental investigation of the mechanics of the quasi-harmonic form of frictional oscillation. Initially the mechanics of stick-slip oscillation will be discussed briefly.

CHAPTER II

1. Introduction

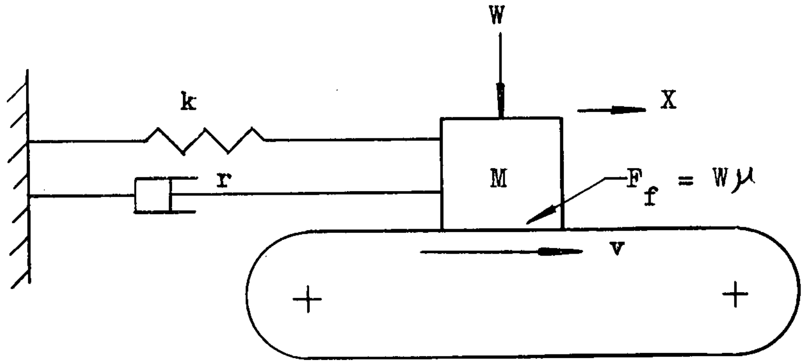

Fig. 1. Diagram of a mass-spring-damping system

Fig. 1. shows schematically the configuration of a typical system which may exhibit friction induced vibration. The elastically restrained slider of equivalent mass M is pressed against the lower surface which is assumed infinitely stiff and is driven at constant velocity 'v'. The motion of the upper surface is produced by the frictional force F_f.

The system damping force is directly proportional to the oscillating velocity (damping coefficient r) and if 'k' is the spring force of the elastic beam, the equation of motion of the system can be written as

$$M \frac{d^2X}{dt^2} + r \frac{dX}{dt} + kX = F_f \tag{1}$$

Where the frictional force may be time dependent or velocity dependent.

Generally the static coefficient of friction μ_s is greater than the kinetic coefficient of friction μ_k. A mechanism of junction growth was suggested by Rabinowicz [8] in explanation of the high value of static coefficient. Further investigation [18] suggested that the increase of static coefficient of friction with time could be expressed mathematically

$$\mu_s = \mu_L + (\mu_u - \mu_L)(1 - e^{-ct}) \qquad (2)$$

Where μ_L and μ_u are respectively the lower and upper limits of the static coefficient and 't' the time of stick. Fig. 2. shows the shape of the curve as expressed by equation (2).

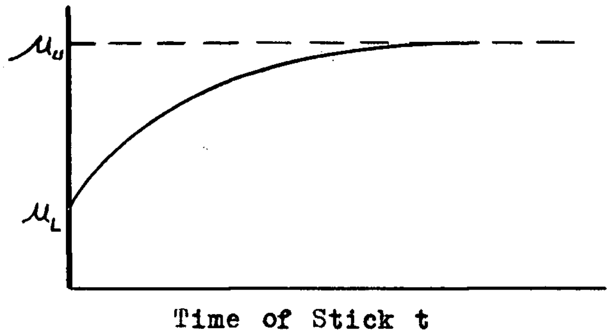

Fig. 2. Relationship between static coefficient of friction and time of stick

During vibration the slider is subjected to a kinetic frictional coefficient which may take a variety of forms (Fig. 3.)

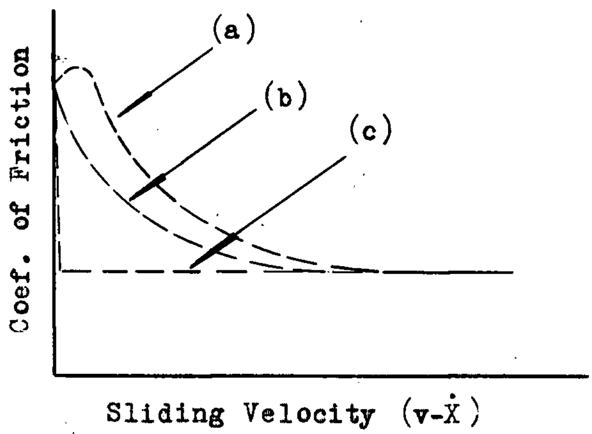

Fig. 3. Various characteristics of frictional coefficient versus sliding velocity

In general, the variation of μ with velocity can be expressed as a function $f(v-\dot{X})$ which is generally known only approximately. In most previous work the analysis of the frictional oscillations has been limited to graphical methods or to linearization of the friction function thus obtaining a linear differential equation.

In the present work an attempt will be made to analyse the friction-velocity characteristic theoretically as well as graphically. The graphical method makes use of the experimental friction-velocity curve directly thus eliminating the complication of finding a suitable function for the curve. In their investigation of frictional relaxation oscillations Dudley and Swift [11] developed a method for investigating the effect of varying the damping coefficient and changing the driven surface velocity.

Let $F = Wf(v-\dot{X})$

Writing $\ddot{X} = \dfrac{d\dot{X}}{dt} = \dot{X}\dfrac{d\dot{X}}{dX}$ and substituting in equation (1) gives

$$\dot{X}\frac{d\dot{X}}{dX} + \frac{r}{M}\dot{X} + \frac{k}{M}X = \frac{F}{M} \tag{3}$$

Rearranging and dividing by $\sqrt{k/M}$, equation (3) becomes

$$\sqrt{\frac{k}{M}}\,X - \frac{F - r\dot{X}}{\sqrt{kM}} = -\dot{X}\frac{d\dot{X}}{dX\sqrt{k/M}} \tag{4}$$

Dividing the frictional force F by $\sqrt{kM}$ gives units of velocity. A curve relating the frictional force and the sliding velocity can then be plotted as shown in Fig. 4. Next, a new axis $\sqrt{\frac{k}{M}}\,X$ of the same dimensions and scale as $F/\sqrt{kM}$ is established with O' as origin and at a distance v away from the $F/\sqrt{kM}$ axis. Finally ABC, the relationship between $\dfrac{F - r\dot{X}}{\sqrt{kM}}$ and the oscillating velocity $\dot{X}$ is obtained by subtracting the system damping effect $r\dot{X}/\sqrt{kM}$ throughout the original frictional force versus velocity curve with O' as origin.

If P represents any momentary condition, so that RO' $= \dot{X}$ and PR $= \sqrt{\frac{k}{M}}\,X$, then it can be easily shown from Fig. 4. that since

$PQ = PR - QR$ and since $QR = \dfrac{F - r\dot{X}}{\sqrt{kM}}$

therefore $PQ = \sqrt{\dfrac{k}{M}}\,X - \dfrac{F - r\dot{X}}{\sqrt{kM}} = -\dot{X}\,\dfrac{d\dot{X}}{dX\sqrt{k/M}}$

also $QS = RO' = \dot{X}$

Thus $\dfrac{PQ}{QS} = \dfrac{-\dot{X}\,\dfrac{d\dot{X}}{dX\sqrt{k/M}}}{\dot{X}} = -\dfrac{d\dot{X}}{dX\sqrt{k/M}}$

Hence SP is the radius vector of the trajectory relating $\dot{X}$ and $\sqrt{\frac{k}{M}}\,X$ at the point P where its tangent is normal to PS, thus a complete trajectory can be developed by drawing successive tangential elements. The trajectory thus obtained will either spiral inwards or outwards ultimately being asymptotic to a closed curve or spiral continually outward and ultimately reaches the $F/\sqrt{kM}$ axis.

Fig. 5. shows a graphical construction of a phase trajectory in which the circle ZZ is for the stable quasi-sinusoidal oscillations.

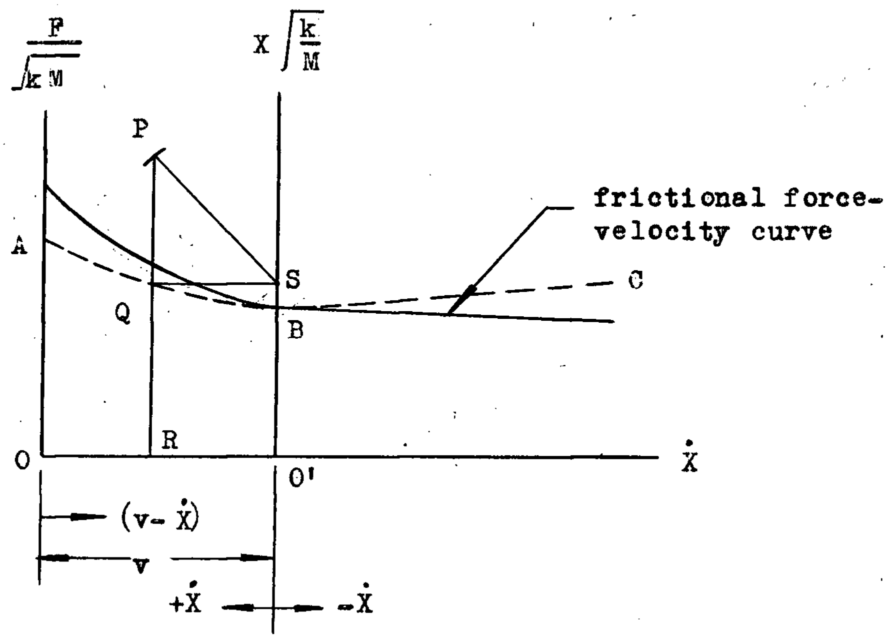

Fig. 4. Graphical construction of phase plane diagram

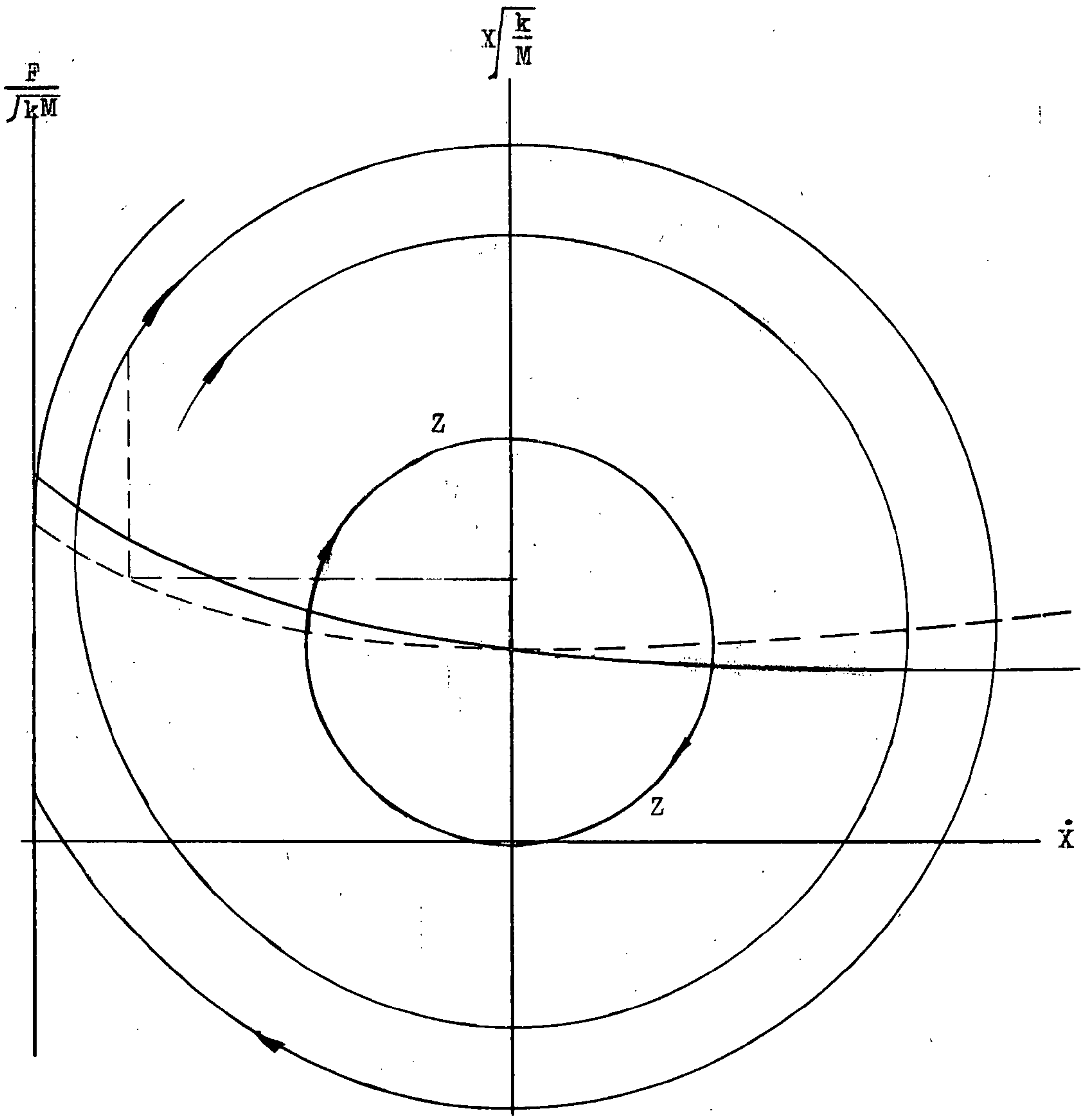

$$\frac{r}{\sqrt{kM}} = 0.1$$

Scale: 1 in = 1 in/sec

Fig. 5. Phase Plane Diagram

The two general forms of friction induced vibration may be investigated analytically using equation (1).

2. Stick-Slip Oscillation

One kind of frictional oscillations is 'stick-slip' sliding which involves periodic sticking as indicated by the displacement-time diagram of Fig. 6. In this type of oscillation the driven surface velocity 'v' is considered to be sufficiently low so that the slider has no difficulty in keeping up with the movement of the lower surface.

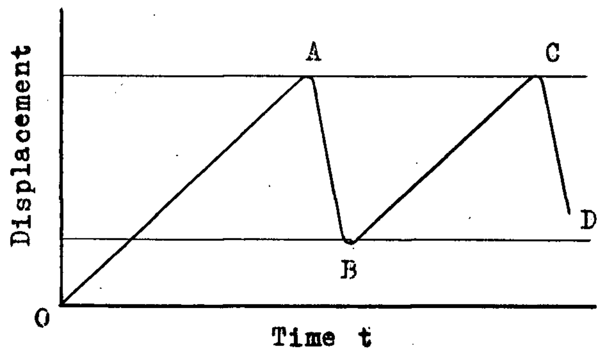

Fig. 6. Displacement-time graph of slider

Consider the slider to be in its equilibrium position and suppose that the slider has remained in that equilibrium position for some time, then as the lower surface moves the slider will stick to the lower surface and move along with it at an absolute velocity $\dot{X} = v =$ constant, i.e. $\ddot{X} = 0$. This portion is shown in Fig. 6. by OA, the equation of motion during this portion is thus

$$rv + kX \leq W\mu_s \tag{5}$$

Up to point A, the static force of friction is capable of withstanding the combined restoring forces consisting of the constant damping force 'rv' plus the spring force 'kX' which increases with time at the rate equal to 'kv'. At A, the spring force plus the system damping force exceeds the static frictional force and slip takes place. The motion of the slider is described by the equation

$$M\ddot{X} + r\dot{X} + kX = W\mu \qquad (6)$$

Owing to the presence of the kinetic frictional force and the system damping force the slider will stop at point B which lies between $+W\mu/k$ and $-W\mu/k$ and the next cycle will follow path BCD.

In some cases, in particular with stick-slip vibrations, the variation of μ with velocity will take the form illustrated by curve (c) of Fig. 3. and described by the equation

$$\mu = \mu_L + S(v - \dot{X}) \qquad (7)$$

Cameron [18] made a very thorough analysis of this linearised case. He based his analysis on equations (6) and (7) and applied boundary conditions at the beginning and at the end of the slip portion. By combining the graphical and analytical methods he derived an equation for the amplitude of oscillation of the form

$$\alpha = X_1 - X_2 = \frac{W}{k}(\mu_S - \mu_L)(1 + e^{-\lambda\pi}) \qquad (8)$$

He then substituted equation (2) for μ_S and let

$$\alpha_m = \frac{W}{k}(\mu_u - \mu_L)(1 + e^{-\lambda\pi})$$

An equation for 'v' was obtained

$$v = \frac{C\alpha}{\ln\frac{\alpha_m}{\alpha_m - \alpha}} \qquad (9)$$

The limit of v as α approaches zero is found by L'Hospital's Rule to be

$$V_c = C\alpha_m$$

where V_c is the critical velocity.

For a given system, equation (9) can be plotted which gives a curve of the form shown in Fig. 7.

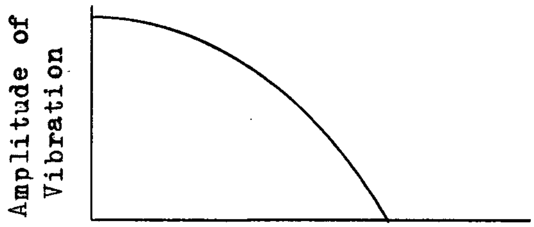

Fig. 7. Graph of amplitude of vibration versus driven surface velocity

3. Quasi-Harmonic Oscillation

Consider the equation of motion

$$M\ddot{X} + r\dot{X} + kX = Wf(v-\dot{X}) \tag{10}$$

Where $f(v-\dot{X})$ is the friction function. When this function is expressed in the form of an equation, all the terms involving $\dot{X}$, $\dot{X}^2$ $\dot{X}^3$ ... etc, can be transferred to the left hand side of the equation, leaving the right hand side with the constant term containing terms in v. If this constant term is represented by e then equation (10) can be written as

$$\ddot{X} + \frac{r}{M}\dot{X} - \frac{W}{M}f(\dot{X}) + \frac{k}{M}X = \frac{W}{M}e \tag{11}$$

Where $f(\dot{X})$ is a function of $\dot{X}$.

Letting $Y = X - \frac{We}{k}$ and $\omega^2 = \frac{k}{M}$

then $\dot{Y} = \dot{X}$, $\ddot{Y} = \ddot{X}$ and $\frac{k}{M}Y = \frac{k}{M}X - \frac{We}{M}$

Substituting these in equation (11) yields

$$\ddot{Y} + \frac{r}{M}\dot{Y} - \frac{W}{M}f(\dot{Y}) + \omega^2 Y = 0 \tag{12}$$

The elimination of the constant term $\frac{W\,e}{M}$ simply means that the slider will vibrate around a new position instead of the original static position with the amplitude of the vibration remaining the same.

Equation (10) can be considered in an alternative way. Taking $|\dot{X}| \ll v$ initially, by Taylor's theorem, referred to by McLachlan [1], we get

$$f(v-\dot{X}) \simeq f(v) - \dot{X}f'(v) + \frac{1}{2}\dot{X}^2 f''(v) - \frac{1}{6}\dot{X}^3 f'''(v)$$

differentiation being with respect to v.
Substituting in equation (10) and dropping the constant term, we get

$$\ddot{Y} + \left(\frac{r}{M} + \frac{W}{M}\left[f'(v) - \frac{1}{2}f''(v)\dot{Y} + \frac{1}{6}f'''(v)\dot{Y}^2\right]\right)\dot{Y} + \omega^2 Y = 0$$

Initially when $\dot{Y}$ is small, and if r, the system damping, is relatively small then the coefficient of $\dot{Y}$ is negative since $f'(v) < 0$, for the case of negative slope of the friction-velocity curve, so that oscillation tends to grow. When the amplitude attains its ultimate value, the coefficient of $\dot{Y}$ is alternately positive and negative, such that the energy supplied from the driven surface is equal to that dissipated. Thus Taylor's expansion demonstrates the importance of the negative slope of the friction-velocity curve.

Equation (12) is a non-linear second order differential equation which can be written in the form

$$\ddot{Y} + \gamma F(\dot{Y}) + \omega^2 Y = 0 \tag{13}$$

where $\gamma F(\dot{Y}) = \frac{r}{M}\dot{Y} - \frac{W}{M} f(\dot{Y})$

An approximate solution of equation (13) may be obtained by the method known as 'slowly varying amplitude and phase' developed by Kryloff and Bogoliuboff [23].

If the non-linear term $\gamma F(\dot{Y})$ is relatively small, a first approximate solution for equation (13) can be written as

$$Y = A \sin\psi \tag{14}$$

where $\psi = \omega t + \Phi$

so $$\dot{Y} = A\omega\cos\psi \tag{15}$$

Supposing the amplitude A and the phase angle Φ are functions of time t and vary slowly with t, then by differentiating equations (14) and (15) with respect to t we get

$$\dot{Y} = \dot{A}\sin\psi + A(\omega + \dot{\Phi})\cos\psi \tag{14a}$$

$$\ddot{Y} = \dot{A}\omega\cos\psi - A\omega(\omega + \dot{\Phi})\sin\psi \tag{15a}$$

from (14a) and (15) we obtain

$$\dot{A}\sin\psi + A\dot{\Phi}\cos\psi = 0 \tag{16}$$

from (13), (14), (15) and (15a) we obtain

$$\dot{A}\cos\psi - A\dot{\Phi}\sin\psi = -\frac{\gamma}{\omega} F(A\omega\cos\psi) \tag{17}$$

and from (16) and (17) gives

$$\dot{A} = -\frac{\gamma}{\omega} F(A\omega\cos\psi)\cos\psi \tag{18}$$

and $\dot{\Phi} = \frac{\gamma}{\omega A} F(A\omega\cos\psi)\sin\psi$ (19)

since A and Φ vary slowly and, as an approximation, one can assume that during one period $2\pi/\omega$ of the trigonometric functions A and Φ remain constant but vary from one period to the other. In other words it can be assumed that the mean values of $\dot{A}$ and $\dot{\Phi}$ over a period 2π in β where $\beta = \omega t$ are sufficiently accurate. Thus from (18) and (19)

$$\dot{A} = -\frac{\gamma}{2\pi\omega}\int_0^{2\pi} F(A\omega\cos\beta)\cos\beta d\beta \qquad (20)$$

$$\dot{\Phi} = \frac{\gamma}{2\pi\omega A}\int_0^{2\pi} F(A\omega\cos\beta)\sin\beta d\beta \qquad (21)$$

In equation (13) the function $F(\dot{Y})$ does not contain any terms of the form Y^2, Y^3 ... etc., hence it follows that all the integrals corresponding to equation (21) are of the form $\int_0^{2\pi}\sin x \cos^n x \, dx$ and since $\int_0^{2\pi}\sin x \cos^n x \, dx = 0$, the integrals corresponding to equation (21) equal to zero, that is Φ is unaffected. Substituting the non-linear function $F(\dot{Y})$ to equation (20) yields an equation for $\dot{A}$.

The amplitude, described as the 'limit cycle amplitude', can be determined by setting $\dot{A} = 0$.

For the purpose of theoretical analysis various forms of friction-velocity curve can be studied. Bristow [9] obtained a number of experimental curves in his investigation of kinetic boundary friction wnich have the general form as shown in Fig. 8. For the following investigation this curve will be used as the basic form of the theoretical friction-velocity curves.

In the present work an attempt has been made to express the friction function in several different forms. One of the earlier attempts was to express the function in the form

$$f(v-\dot{X}) = \frac{a}{(v-\dot{X}) + b} + c$$

Owing to its simplicity in form, its accuracy for fitting the experimental curve is limited.

It was later decided that the friction function would be fitted by a polynomial. Knowing the approximate shape of the friction-velocity curve Newton's method [24], making use of a difference table, was used for obtaining the polynomial. In order to obtain an adequate fit of the actual curve with the polynomial, all the figures in the right hand side column of the table should be closely equal. The number of columns presented in the table determines the degree of the polynomial.

For a 6th degree polynomial the friction function will have the form

$$f(v-\dot{X}) = C_1(v-\dot{X})^6+C_2(v-\dot{X})^5+C_3(v-\dot{X})^4+C_4(v-\dot{X})^3+C_5(v-\dot{X})^2+C_6(v-\dot{X})+C_7 \qquad (22)$$

Expanding the bracketed terms and collecting coefficients gives the polynomial in the form

$$F(\dot{X}) = e_1\dot{X}^6 - e_2\dot{X}^5 + e_3\dot{X}^4 - e_4\dot{X}^3 + e_5\dot{X}^2 - e_6\dot{X} + e_7$$

where
$$e_7 = (C_1v^6 + C_2v^5 + C_3v^4 + C_4v^3 + C_5v^2 + C_6v + C_7)$$
$$e_6 = (6C_1v^5 + 5C_2v^4 + 4C_3v^3 + 3C_4v^2 + 2C_5v + C_6)$$
$$e_5 = (15C_1v^4 + 10C_2v^3 + 6C_3v^2 + 3C_4v + C_5)$$
$$e_4 = (20C_1v^3 + 10C_2v^2 + 4C_3v + C_4)$$

$$e_3 = (15C_1v^2 + 5C_2v + C_3)$$
$$e_2 = (6C_1v + C_2)$$
$$e_1 = C_1$$

Substituting these values in the equation for A we get

$$A = 0$$

and

$$\frac{5}{8} e_2(A\omega)^4 + \frac{3}{4} e_4(A\omega)^2 + \frac{r+We_6}{W} = 0 \tag{23}$$

Thus the amplitude will be either $A = 0$ or A equals one of the roots of equation (23).

Because of the extensive calculations required, particularly if a polynomial of a degree higher than the sixth was required for an accurate representation of the friction function, the calculations were performed by the computer. The computer program was divided into three sections. The first section used Newton's method for obtaining coefficients of the polynomial for the friction function. The second section gave values of this newly established function at equal intervals so that a theoretical curve could be plotted to check with the original curve. The last section involved the calculation of the e_1, e_2, ... etc. for values of v starting from 0 in/sec in increments of 0.5 in/sec. The program also solved for the roots of the amplitude polynomial.

The results obtained from the computer program showed that the values of e_1, e_2, ... etc. were very small, thus the assumption that the non-linear term $\gamma F(\dot{Y})$ of equation (13) is relatively small was substantiated. The γ function derived from these computations was less than one.

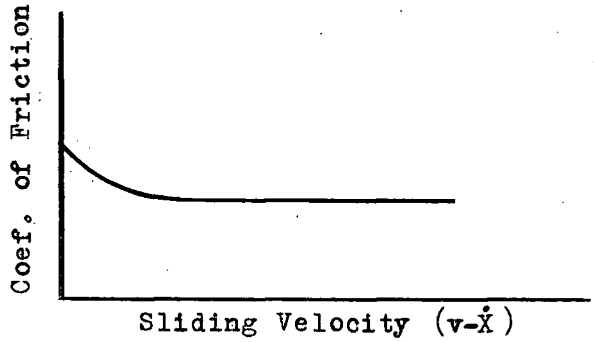

Fig. 8. Adopted form of theoretical friction-velocity curves

In Fig. 9. four theoretical curves are shown. Curves (A) and (B) are identical except that (B) is shifted vertically downward for a frictional coefficient value of 0.18. Curve (C) has the same static coefficient of friction as curve (A) but the flattening point of its negative slope occurs at a lower velocity than that of the curve (A). Curve (D) has a lower static coefficient of friction and its negative slope region ends at an earlier stage than that of the other three.

10th degree and 12th degree polynomials were used to fit these curves. Results from the computations showed that curves (A) and (B) should give rise to the same magnitude of frictional oscillations, and the oscillations should terminate at the same velocity. These findings justify the elimination of the constant term in equation (11). The results also show that the amplitude of the frictional oscillations for curves (A), (C) and (D) increases at approximately the same rate as the velocity increases but the vibration terminates or becomes unstable at different velocities. Further study of the results show that these termination points are closely related to the flattening point of the negative slope of the curves.

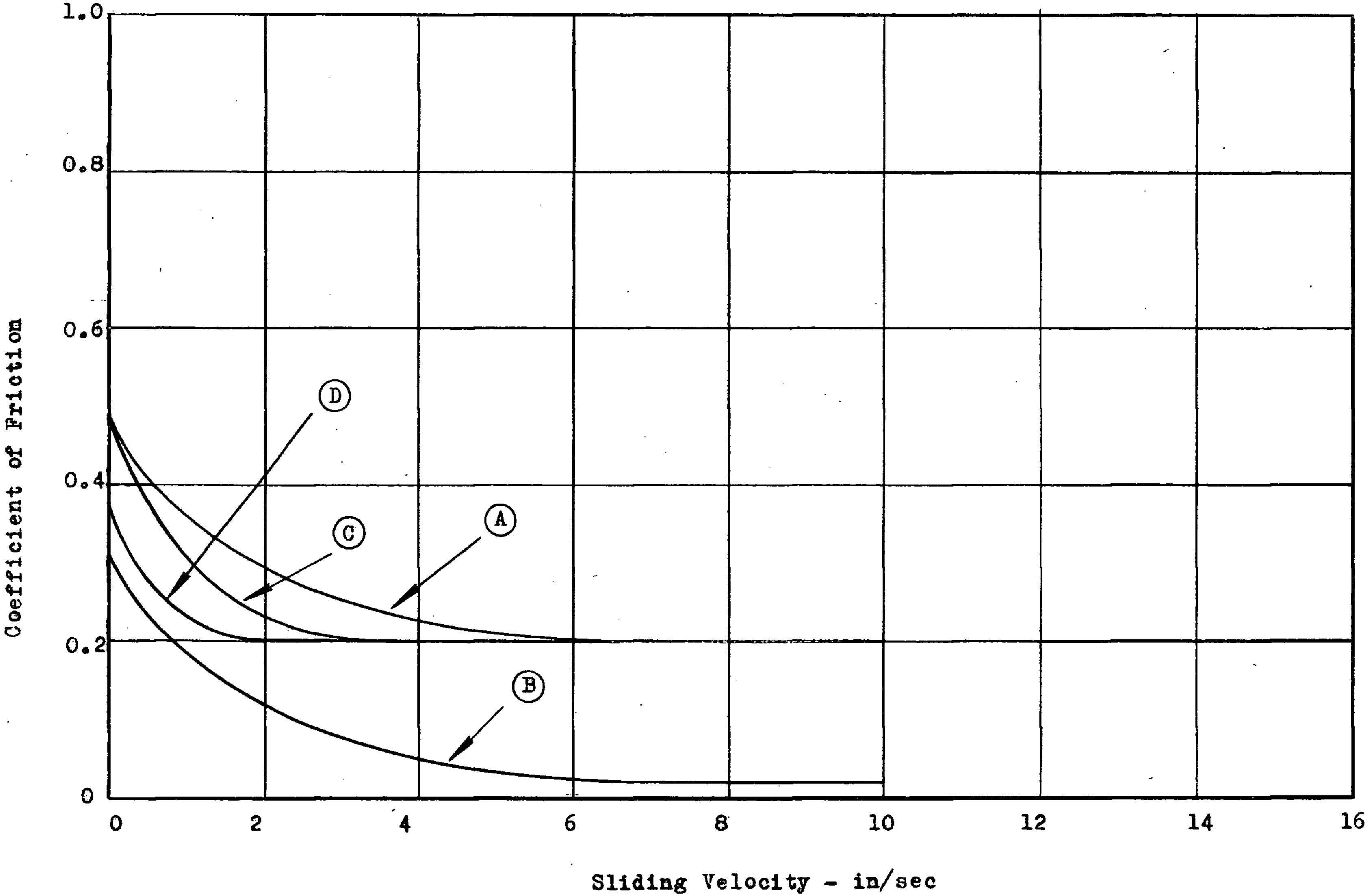

Fig. 9. Theoretical Friction - Velocity Curves

The effect of increasing the damping coefficient was investigated theoretically. The results showed that for the same friction-velocity curve the frictional oscillation became unstable at an earlier stage with a higher damping coefficient. The word 'unstable' used in connection with the oscillation refers to inconsistency of amplitude. The results are plotted in Figs. 10. and 11.

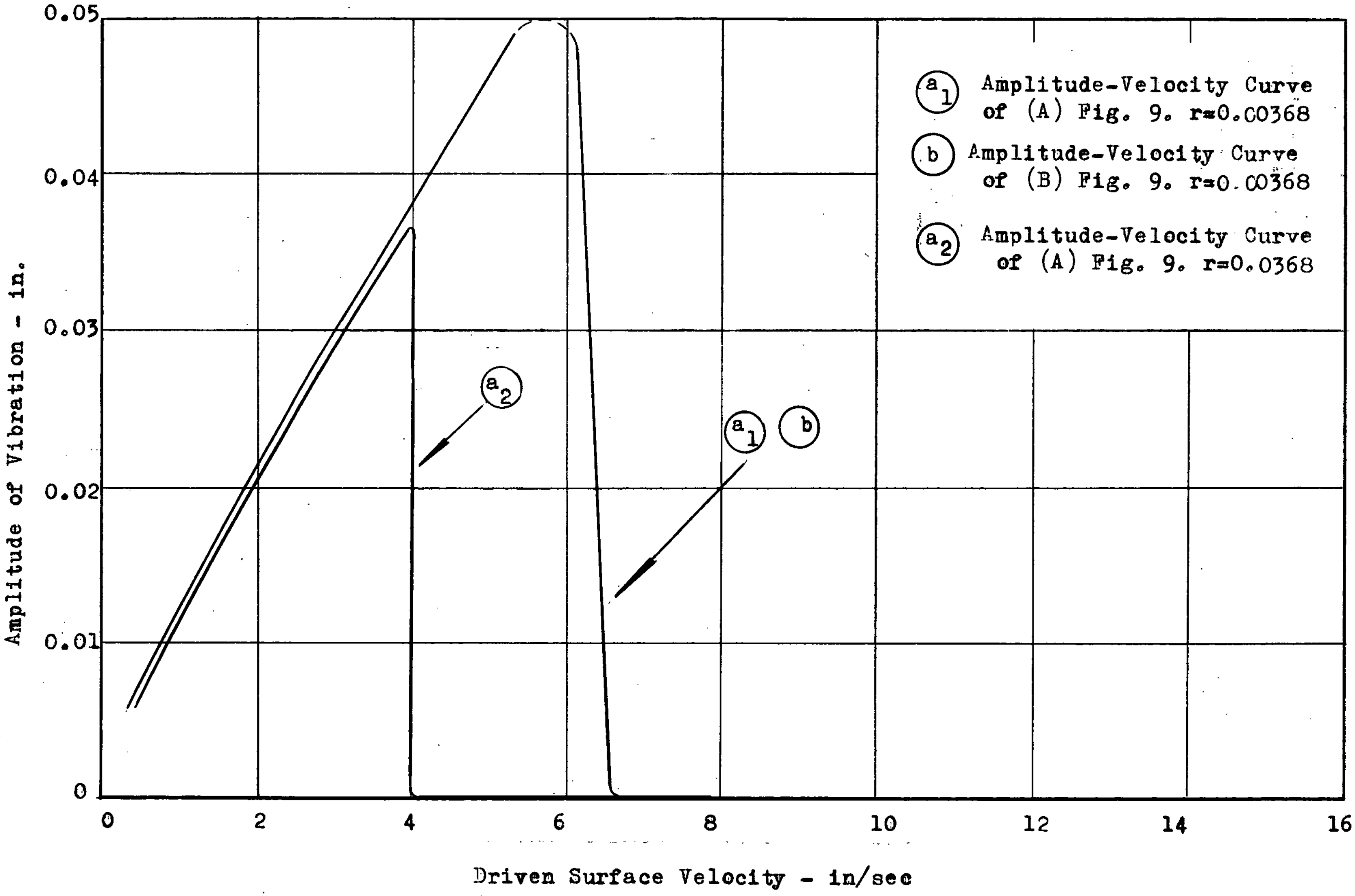

Fig. 10. Graph of Amplitude of Vibration Versus Driven Surface Velocity - Theoretical

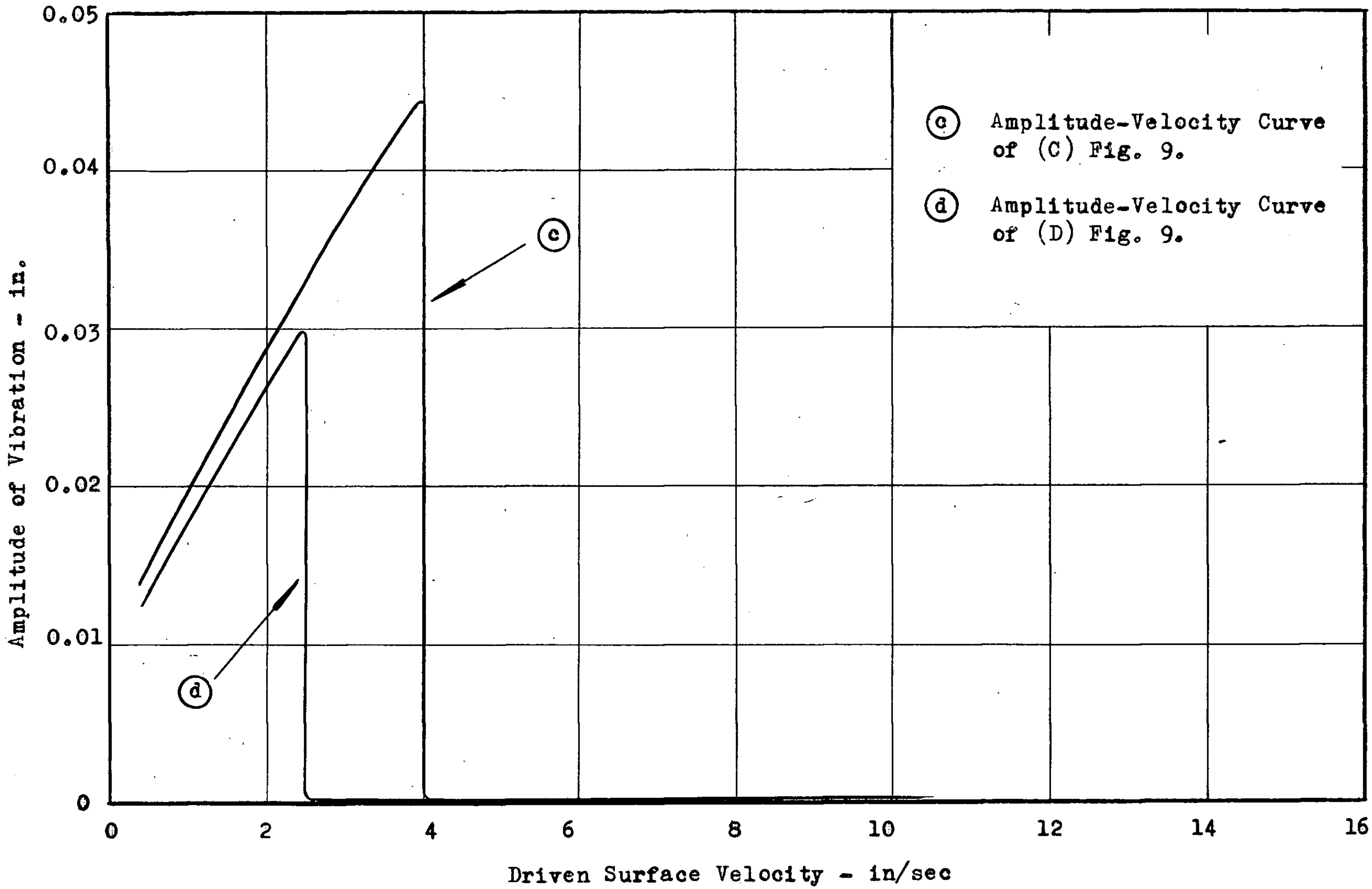

Fig. 11. Graph of Amplitude of Vibration Versus Driven Surface Velocity - Theoretical

CHAPTER III

1. Vibration Apparatus

The vibration apparatus is basically the same as that used previously by Pomeroy [25] for friction and wear investigations. A general view of the vibration apparatus and the other instruments is shown in Fig. 12. and a detailed drawing of the apparatus is shown in Fig. 13.

The essential parts of the vibration apparatus are a rotating disc as the lower surface and a slider as the upper surface. The slider is attached to a semicylindrical slider mount which forms part of a self-aligning joint. The joint allows the slider to rotate in two orthogonal directions hence ensuring that the slider bears evenly on the rotating disc. The self-aligning joint is fixed to a steel beam which forms the elastic supporting system of the slider. A steel bar to which the elastic beam is cantilevered pivots on two ball bearing journals. Load is applied to the steel bar through a pulley system. A lead screw passing through the bottom of the base provides movement of the entire assembly, thus permitting adjustment of the radial position of the slider on the rotating disc.

The driving unit consists of a variable speed servo-controlled d.c. motor. The motor is coupled to a worm gear reducer which in turn drives the rotating disc through a roller chain drive and a set of bevel gears. The speed range of the rotating disc is from 0 to 144 r.p.m.

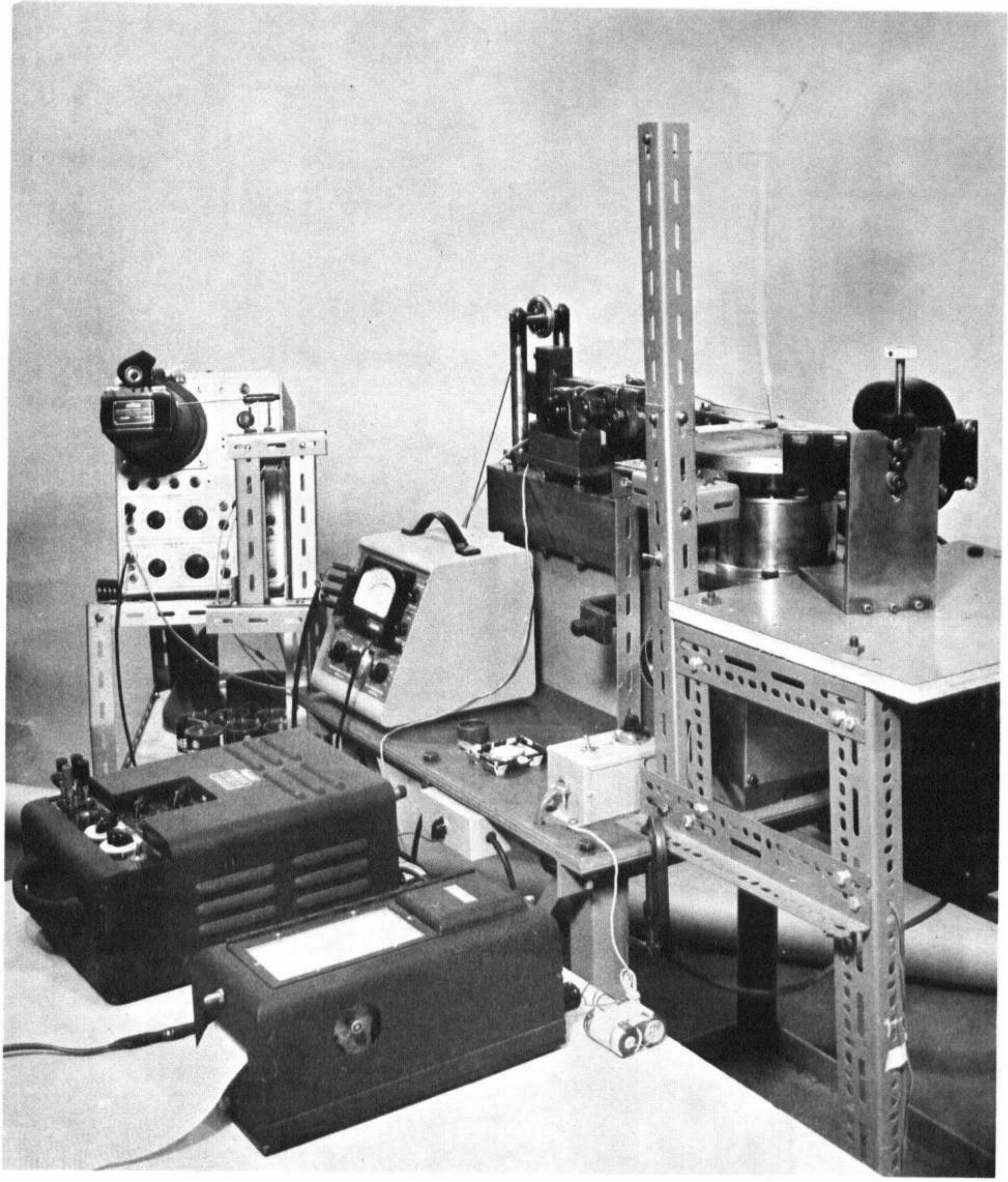

Fig. 12 General Arrangement of Instruments and Vibration Apparatus.

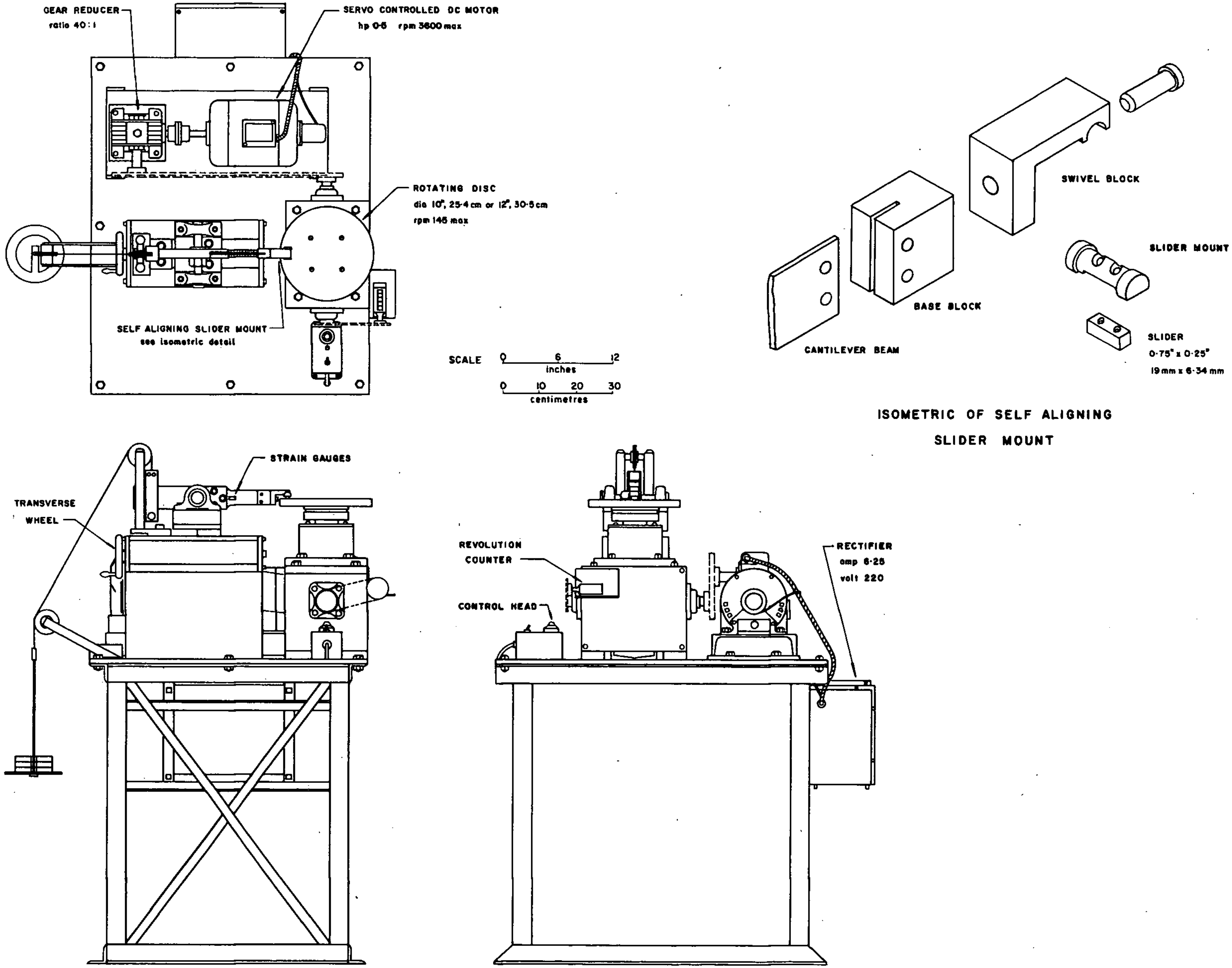

Fig. 13. Drawing of Vibration Apparatus

2. Instrumentation

Instruments were designed in order to determine displacement and velocity of the slider movement during frictional oscillations. The system is shown diagrammatically in Fig. 14.

A. Measurement of Displacement

The elastic beam had 500 ohm strain gauges (SR-4, Type C-7) cemented to each side, which were used to measure the displacement of the slider. The two strain gauges together with two 500 ohm resistors formed a four arm bridge circuit which was connected to a Bridge Amplifier Meter (Model BAM-1) and a Brush Universal Analyser (Model BL 320) by way of a four pole rotary switch. This rotary switch provided a means for the rapid change from the Bridge Amplifier Meter to the Universal Analyser or vice versa.

The Brush Universal Analyser was connected to one channel of a two channel Brush oscillograph (Model BL 202) while the Bridge Amplifier Meter was connected to the lower beam of a Dual Beam Oscilloscope (Tektronic, Type 502), so that the displacement-time curve of the slider during frictional oscillations could either be obtained from the oscillograph as a chart record or could be observed and photographed from the screen of the oscilloscope.

It was observed that the 2,000 cps frequency from the oscillator circuit inside the Universal Analyser was picked up by the Bridge Amplifier Meter, this behaviour was attributed to mutual inductance effect within the rotary switch. In order to compensate for this effect, an on-off switch was installed in the oscillator circuit

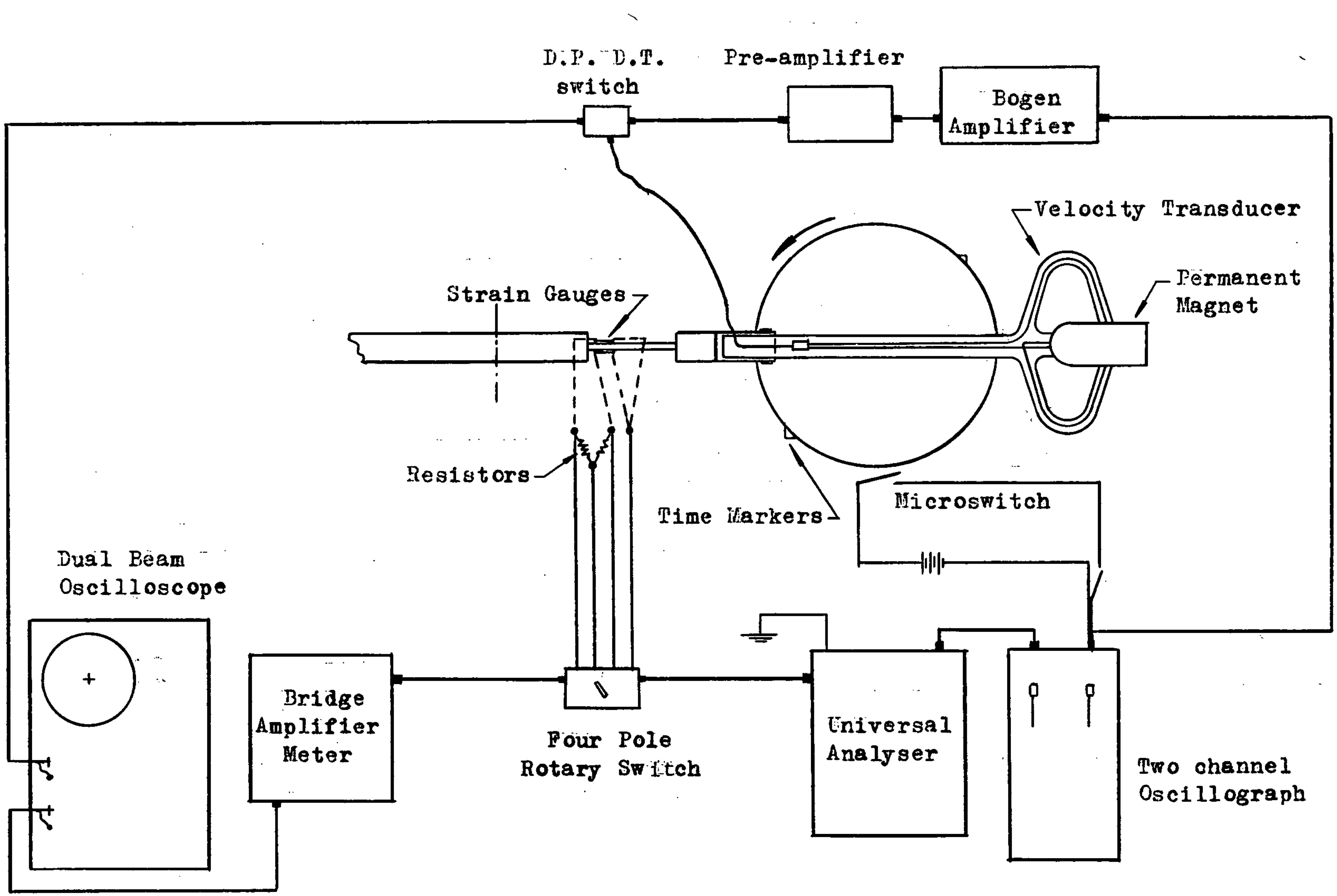

Fig. 14. Diagrammatic View of Instruments

which rendered the oscillator circuit inactive when the Bridge Amplifier Meter and the Oscilloscope were in operation, but at the same time kept the Universal Analyser in stand-by position.

B. Measurement of Velocity

The velocity of the slider was measured by an electromagnetic transducer. A specially shaped frame made from 1/8 in. thick phenolic board as shown in Fig. 15. was firmly attached to the top side of the self-aligning joint. Six coils of enamelled wire were cemented on the frame. A 5,000 gauss permanent magnet was positioned such that when frictional oscillations occurred the conductors cut across the field between the two poles of the magnet. The voltage generated was proportional to the velocity of oscillation of the conductors and the slider. The frame together with the conductors weighed only 4 oz and its cross section was rigidly reinforced thus ensuring that subsidiary vibrations did not occur.

A velocity-time curve was obtained by connecting the conductors to the upper beam of the dual beam oscilloscope. With suitable calibration and gain adjustment, a displacement-velocity phase plane diagram could be obtained from the oscilloscope. Details of these calibrations are given in Appendix A. The velocity-time curve could also be obtained as a chart record from the second channel of the Brush oscillograph. However, for this purpose the very small voltage generated by the velocity transducer was amplified in a single stage pre-amplifier and a Bogen Amplifier (Model PDR).

C. Time Marker

The other channel of the oscillograph was connected to a time marker. A microswitch was mounted close to the rotating disc, so that each time the switch was closed by the reference pointers attached to the disc periphery a voltage pulse was generated which caused the oscillograph pen to deflect, thus providing reference orientations every disc revolution. The time marker was also used during the photography of the oscilloscope traces. For comparison purposes it was necessary to take photographs at the same location during each revolution of the disc. To achieve this result the voltage pulse energised a solenoid which released the spring of a specially designed camera shutter (Fig. 16.).

3. Specimens

The experiments were performed using a disc flame cut from S.A.E. 1030 steel. After annealing the disc had a hardness of Rockwell B64. The finished size of the disc was 10 in. diameter and 3/4 in. thick. Sliders were prepared from identical material and were 3/4 in. x 1/4 in. with an effective surface of 1/4 in. x 1/4 in.

Many methods for preparing the surfaces were tried, these included lathe machining, polishing with emery paper, grinding and lapping. The fine machining method soon proved to be unsuccessful, since damage of the surfaces resulted soon after the test started so that further study of friction-velocity characteristic was prevented. Polishing with emery paper was investigated. After machining the disc, 220-A Tufbak emery paper was applied to the surface

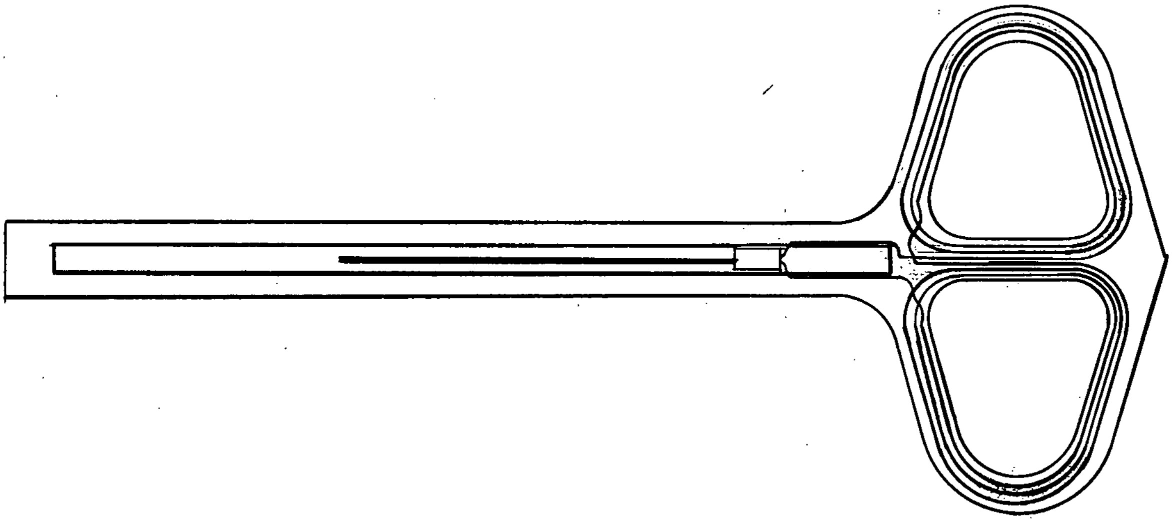

Fig. 15. Velocity Transducer

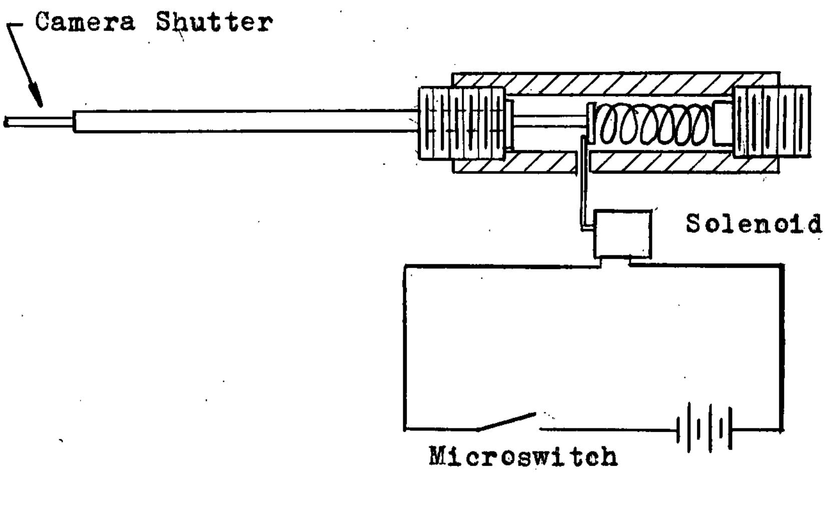

Fig. 16. Solenoid Operated Camera Shutter

while the disc was rotating at high speed, followed by grade 400-A Tufbak for final finishing. A Brush Surfindicator (Model BL 110) was used to find the average roughness of the finished surfaces. Chart records of surface profile were obtained from an oscillograph connected to the Surfindicator through a Brush Amplifier (Model BL 905). The finished surfaces when prepared by the above polishing method had a roughness of 7 microinches R.M.S. However, tests revealed that either heavy tearing resulted or inconsistent results were obtained. Surface profiles before and after the test are shown in Fig. 29. Appendix D. The most satisfactory surfaces were prepared by grinding, followed by a lapping operation with fine carborundum using a cast iron lap. The roughness of the surfaces prepared by this method was about 40 microinches, with surface profiles as shown in Fig. 30. Appendix D.

The curvature effect of a relatively long slider on a 10 in. dia. disc might be negligible when used in connection with friction and wear investigation without vibration. However, considerable effect could arise when frictional oscillations occur, in particular, when the curvature of the slider movement is in the opposite sense to the curvature of the slider track. In order to minimise this effect the slider was designed to give an effective bearing surface of 1/4 in. x 1/4 in. thus keeping the length to a minimum.

CHAPTER IV

1. Test Technique

Preliminary tests were conducted to study the effect of the load and driven surface velocity on the friction-velocity characteristic. It was found that heavy loads tended to accelerate the damage of the surfaces. It was found that loads between 1.968 lb to 3.936 lb normal force on the slider were the most suitable for the present work. The control head for the servo-motor permitted speed increments as small as 0.147 rpm. The total speed range of the rotating disc is 0 to 144 rpm. Preliminary tests revealed that no significant results were observed at speeds above 50 rpm and inconsistent movement of the disc resulted at speed lower than 1 rpm. Therefore it was decided that tests would be carried out within the speed range from 1 rpm to 50 rpm.

For the tests, speed increments of 0.735 rpm were used between 1 rpm and 12 rpm and above 12 rpm the speed increment was raised to 2.94 rpm. Three tracks on each side of the disc were used at 8 in., 8-3/4 in. and 9-1/2 in. diameter respectively. However, in order to minimise the curvature effect the innermost track was used for preliminary tests only.

In order to find the coefficient of friction, the elastic system was calibrated by applying a known force to the slider in the direction of slider motion and measuring the deflection of the slider. Details of the calibration is given in Appendix B.

All the electronic instruments were switched on half an hour prior to each test, thus giving sufficient time for the instruments to become stable. The electronic instruments were then balanced and calibrated. The sliding surfaces were washed with trichlorethylene and ethyl-alcohol just before the test started.

All the tests were carried out on freshly prepared surfaces. After some experimentation it was found that a run-in period was required before the quasi-harmonic oscillation appeared.

2. Experimental Results and Analysis

Oscillograph chart records were taken at intervals of run-in distance and from these chart records friction-velocity and amplitude-velocity curves were derived. The variation of the shape of the friction-velocity curves with the total distance run is illustrated by Fig. 17. It will be noted that there is a growth in coefficient of friction in the low speed region as the run-in distance increases and eventually all these curves have approximately the same value in the high speed region. This growth in coefficient of friction ceases and in some cases may even show reduced friction values after a certain run-in distance has been attained. In Fig. 18. the general trend of this rise and fall of the coefficient of friction versus run-in distance is shown.

As the run-in distance increases the coefficient of friction in the low speed region of the friction-velocity curve increases and a negative characteristic begins to form. At this stage, frictional oscillations commenced. Once the oscillation appeared, it was found to be stable over a range of lower surface velocities.

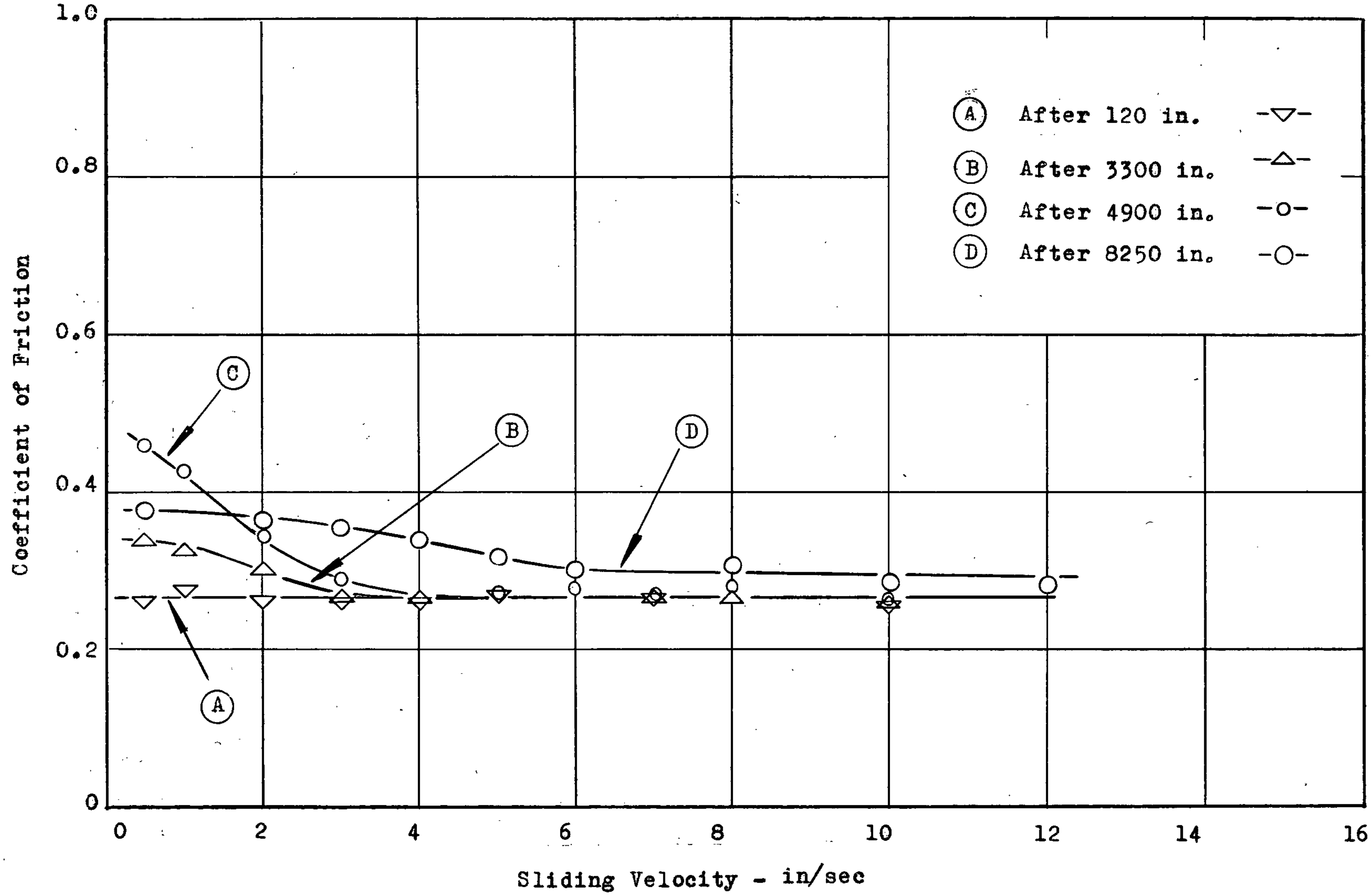

Fig. 17. Graph of Coefficient of Friction Versus Sliding Velocity during Various Run-in Period

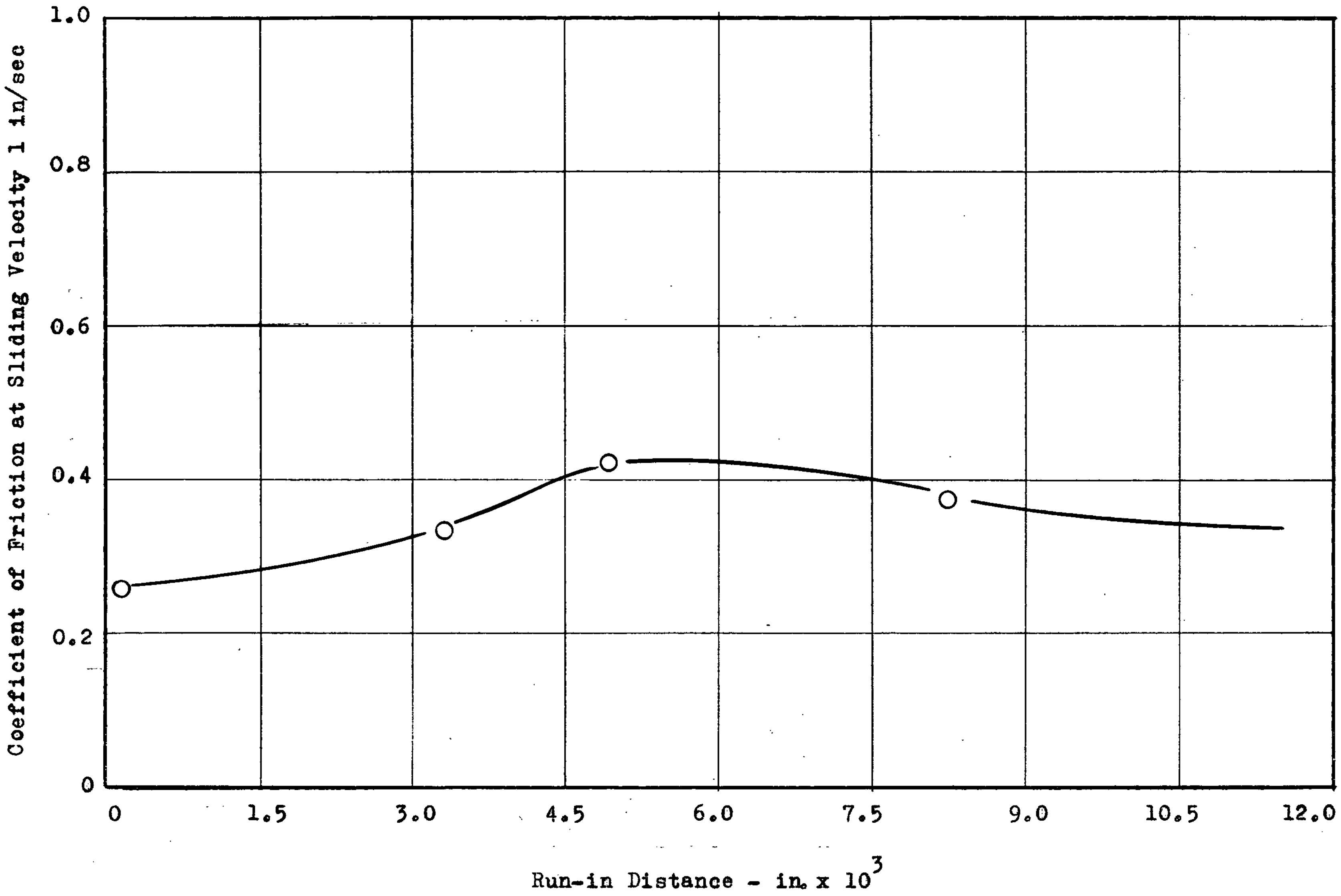

Fig. 18. Graph of Run-in Distance Versus Coefficient of Friction

The amplitude of these oscillations increased as the disc velocity increased until a critical velocity was achieved. Further increase in velocity reduced the amplitude of the oscillation abruptly. In Figs. 19. to 22. amplitude versus driven surface velocity are plotted on the same graph as the friction-velocity curves. It will be noted that the point where unstable oscillations begin to appear almost coincides with the point where the negative slope of the friction-velocity curve flattens out. The corresponding chart records are shown in Figs. 23. and 24. Chart records were normally taken at chart speed of 25 mm/sec, however, in order to obtain a more detailed picture of the shape of the frictional oscillation, a chart speed of 125 mm/sec was used. A typical recording at the higher chart speed is shown in Fig. 25c. Figs. 25a. and 25b. show some irregular stick-slip oscillations obtained from a preliminary test on resin coated surfaces at a very low driven surface velocity and with no run-in distance.

When steady frictional oscillations were observed, the signals from the strain gauges and from the velocity transducer were switched to the oscilloscope which had been calibrated and centred prior to the start of the test. The displacement of the oscillations was displayed on the lower beam of the vertical plates and the velocity of the oscillations was displayed on the upper beam of the vertical plates. The horizontal plates served as time base. Thus a displacement-time curve as well as a velocity-time curve would be observed on the oscilloscope screen. By transferring the upper beam, that is the velocity signals, to the horizontal plates and keeping the lower beam for the displacement signals, a phase plane plot could be obtained. Figs. 26. and 27. show photographs of phase plane

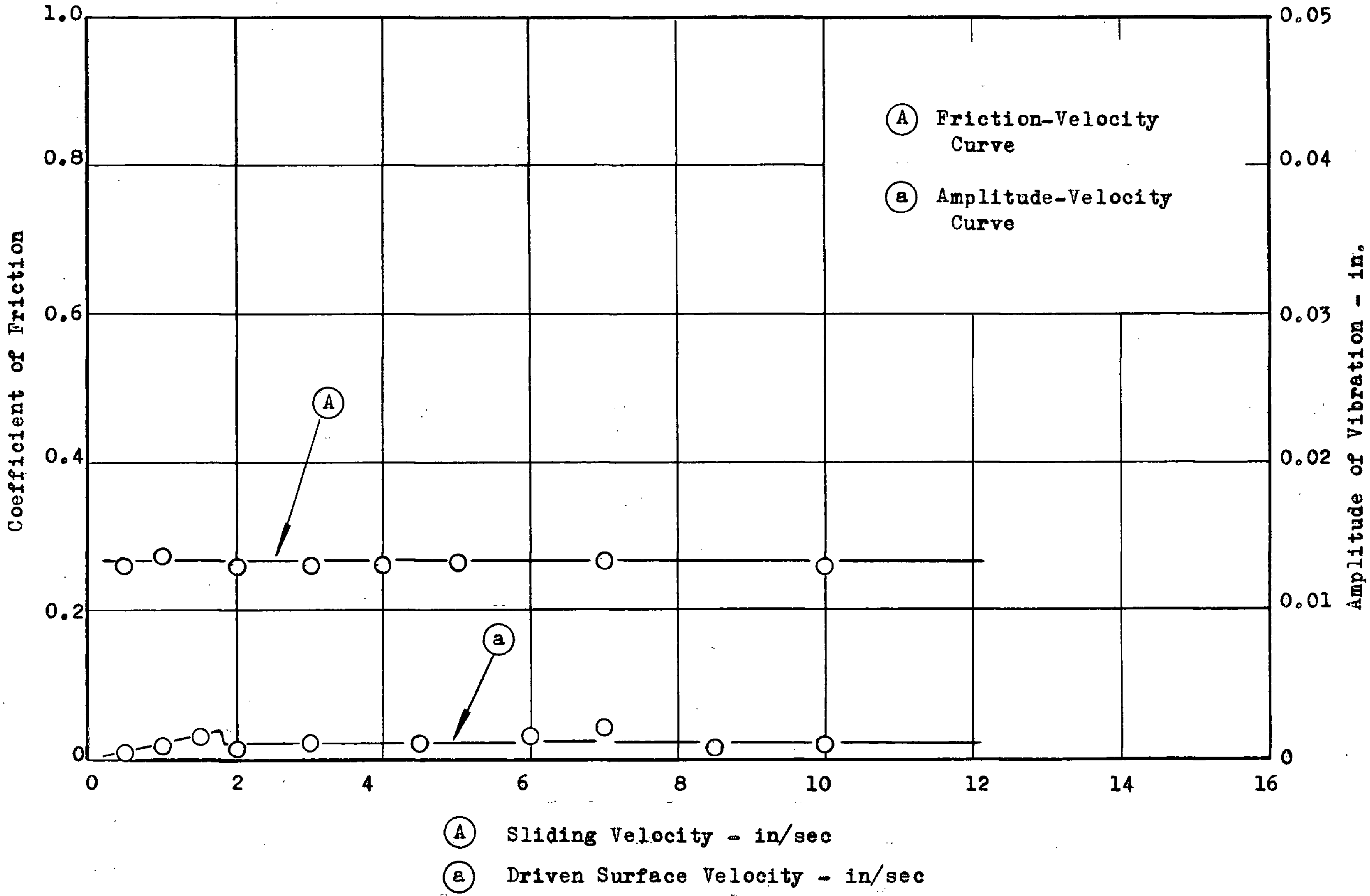

Fig. 19. Graph of Friction-Velocity and Amplitude-Velocity Curves - A

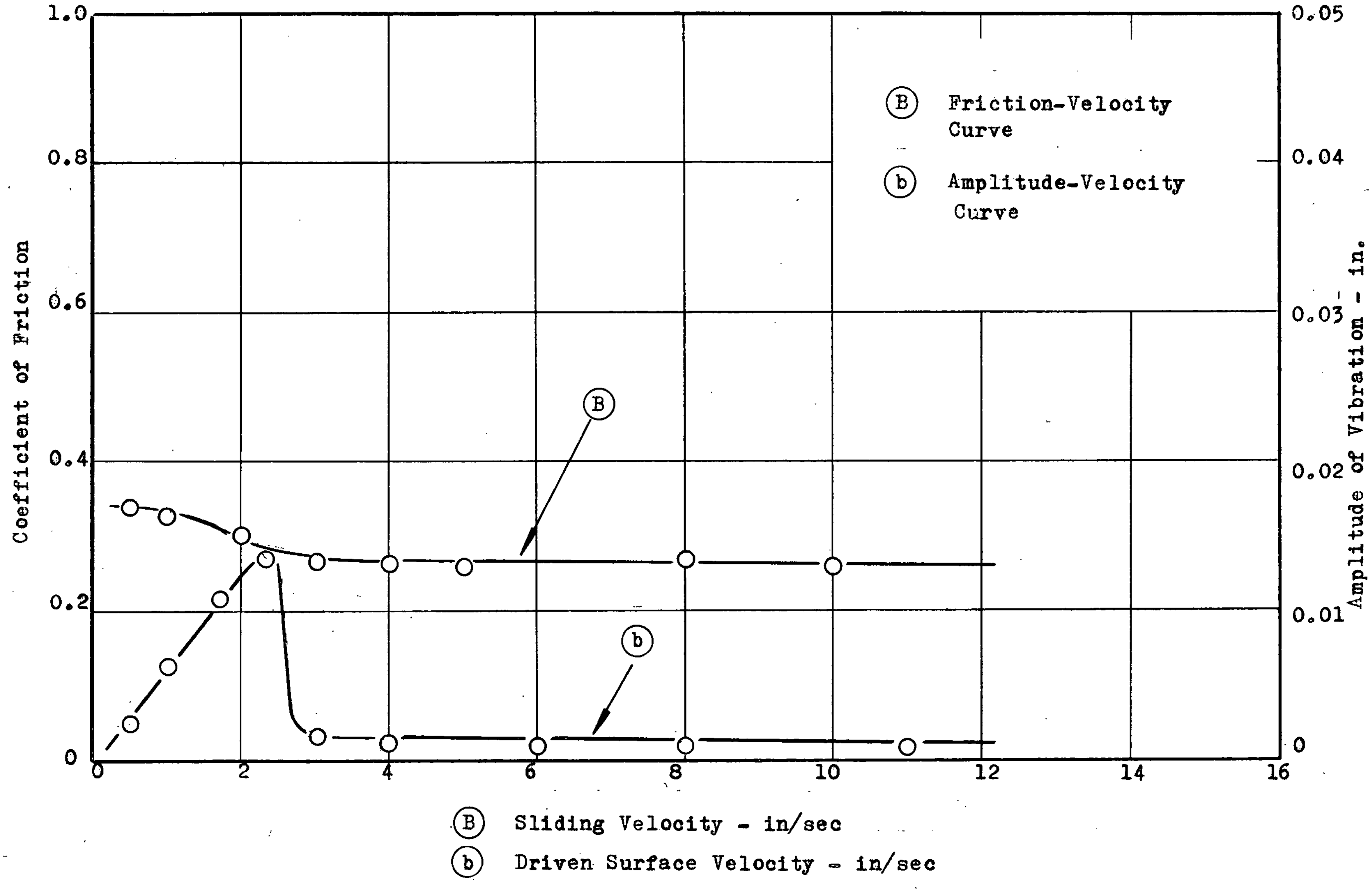

Fig. 20. Graph of Friction-Velocity and Amplitude-Velocity Curves - B

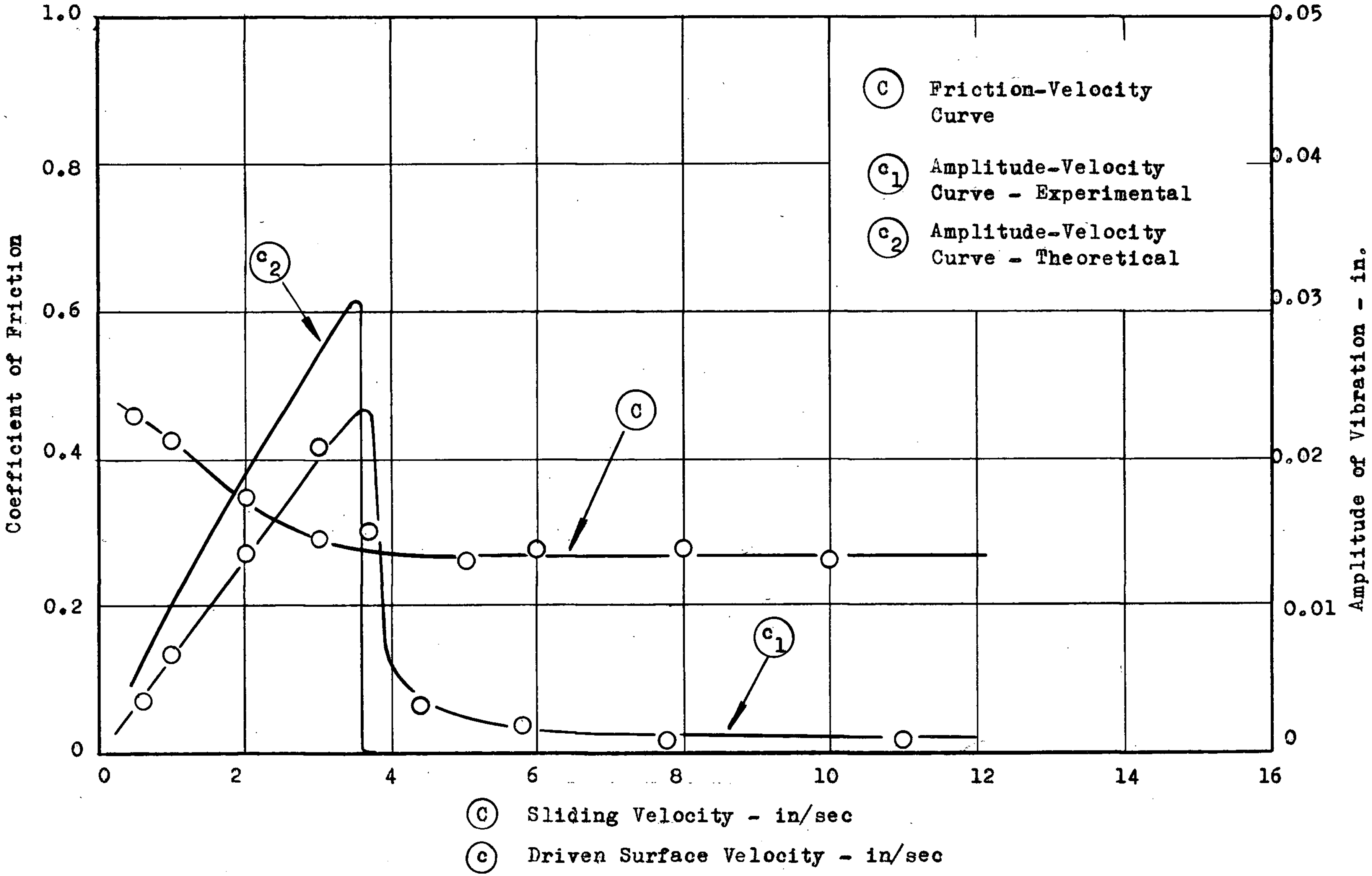

Fig. 21. Graph of Friction-Velocity and Amplitude-Velocity Curves - C

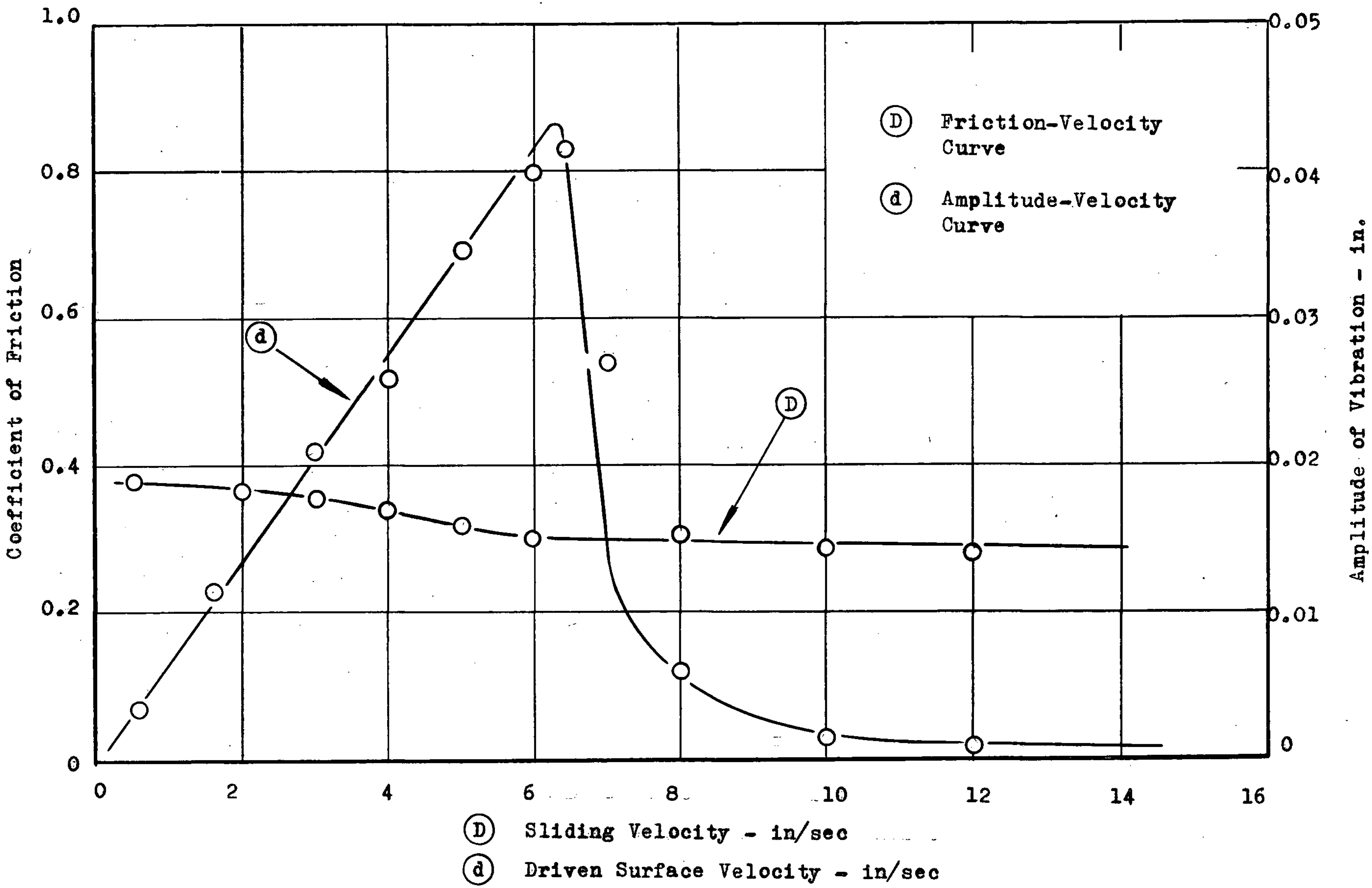

Fig. 22. Graph of Friction-Velocity and Amplitude-Velocity Curves - D

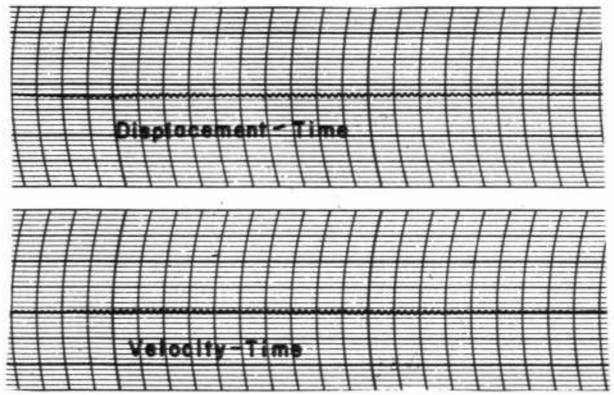

(a) Run-in = 0 in.
Disc Speed = 1 in/sec

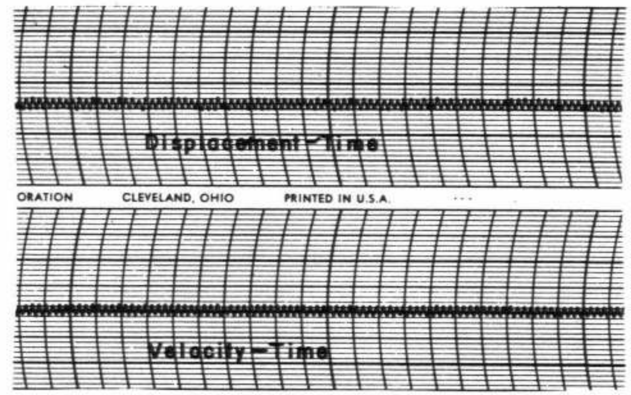

(b) Run-in = 2150 in.
Disc Speed = 0.68 in/sec

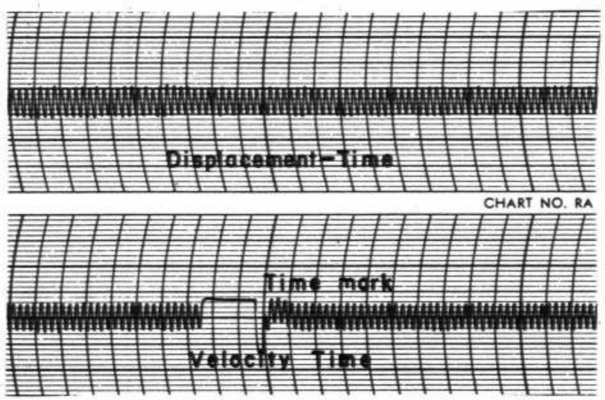

(c) Run-in = 2400 in.
Disc Speed = 1.37 in/sec

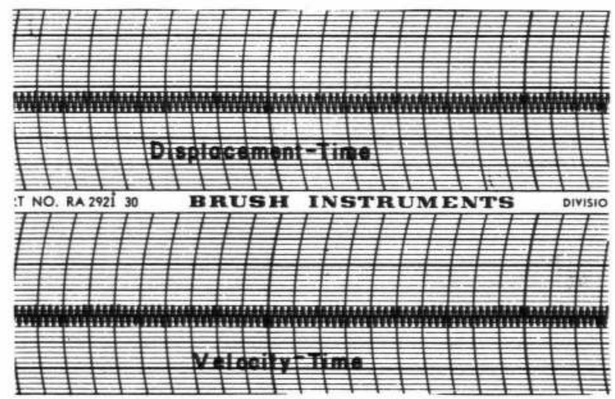

(d) Run-in = 3350 in.
Disc Speed = 1 in/sec

Chart Speed = 25 mm/sec

Displacement; 1 line = 0.00332 in.

Fig. 23. Oscillograph Trace During Frictional Oscillation

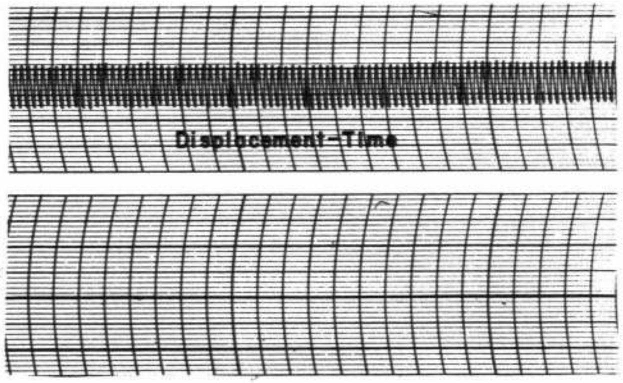

(a) Run-in = 4950 in.
Disc Speed = 2.03 in/sec

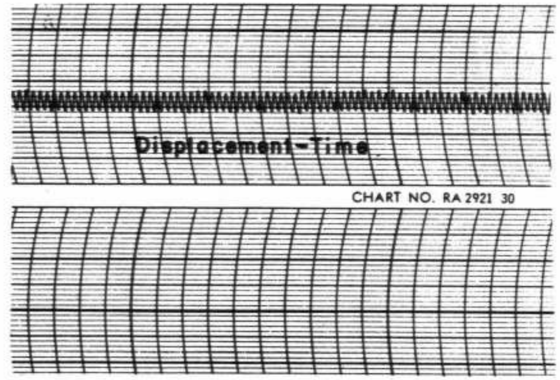

(b) Run-in = 8250 in.
Disc Speed = 0.95 in/sec

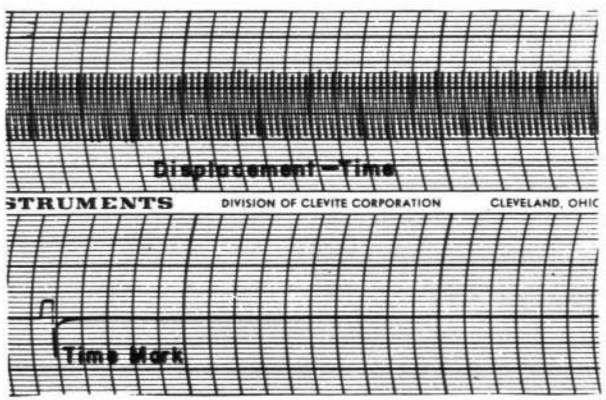

(c) Run-in = 8250 in.
Disc Speed = 3.02 in/sec

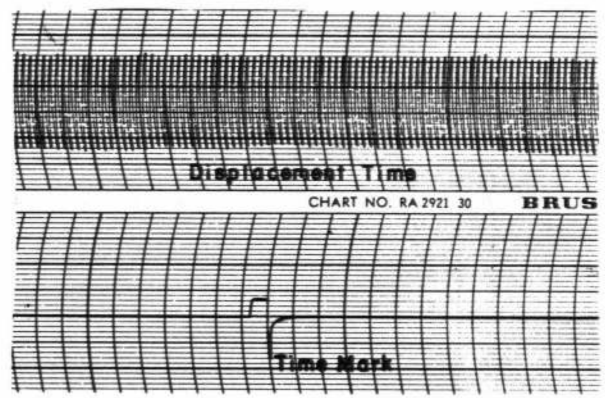

(d) Run-in = 8250 in.
Disc Speed = 4.38 in/sec

Chart speed = 25 mm/sec

Displacement; 1 line = 0.00332 in.

Fig. 24. Oscillograph Trace During Frictional Oscillation

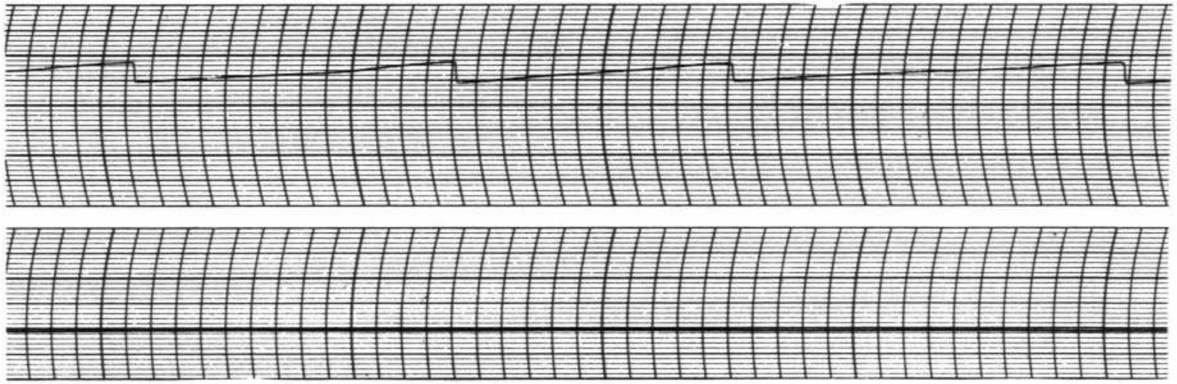

(a) Irregular Stick-Slip Oscillation
Resin Coated Surfaces

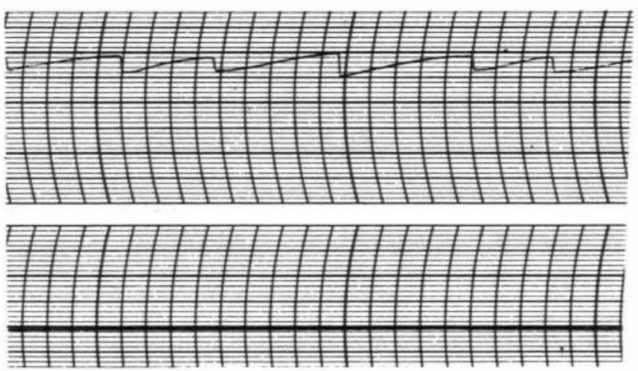

(b) Irregular Stick-Slip Oscillation
Resin Coated Surfaces

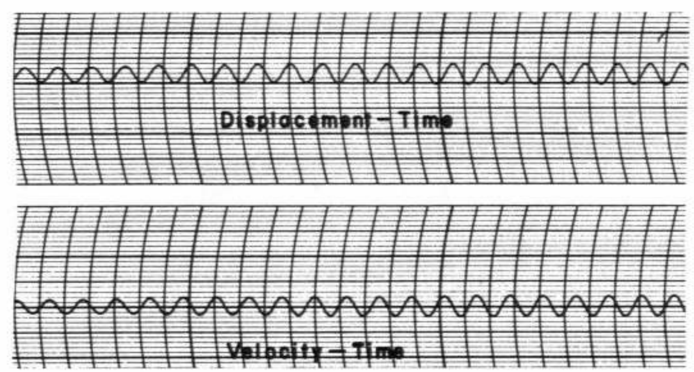

(c) Quasi-Harmonic Oscillation
Dry Surfaces

Chart speed = 125 mm/sec

Fig. 25. Oscillograph Trace During Frictional Oscillation

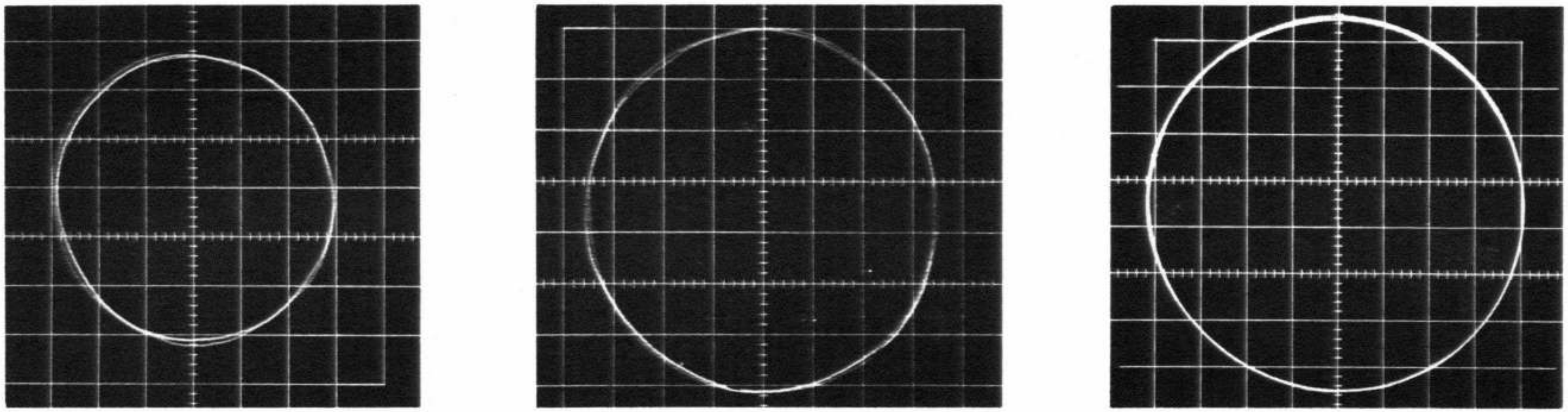

(a)

Normal Force = 1.968 lb
Disc Speed = 4.0 in/sec
Ref.: Fig. 22.

(b)

Normal Force = 1.968 lb
Disc Speed = 4.5 in/sec
Ref.: Fig. 22.

(c)

Normal Force = 2.952 lb
Disc Speed = 6.5 in/sec
Lubricated Surfaces

Scale Factors :	Displacement	1 Div. = 0.0018 in
	Velocity	1 Div. = 0.216 in/sec

Fig. 26. Oscilloscope Trace of Phase Plane Diagrams

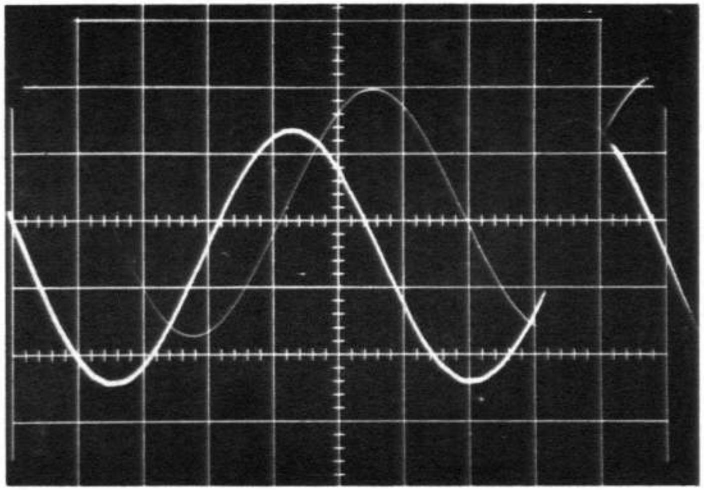

(a) Normal Force = 2.952 lb
Disc Speed = 6.0 in/sec
Lubricated Surfaces

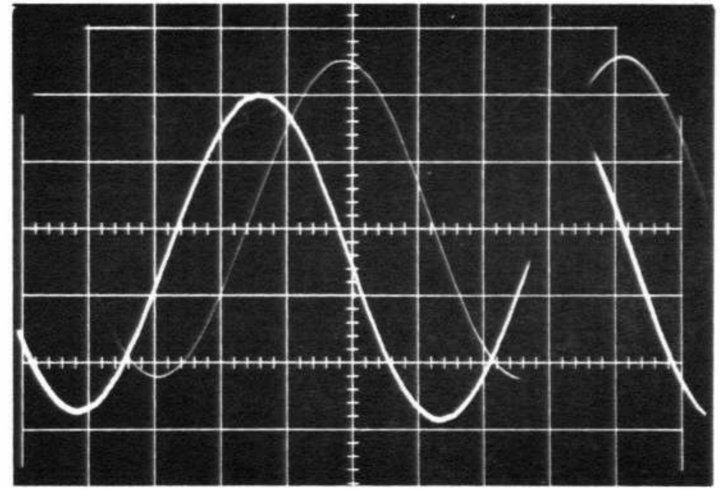

(b) Normal Force = 2.952 lb.
Disc Speed = 6.4 in/sec
Lubricated Surfaces

Scale Factors :	Displacement	1 Div. = 0.00178 in
	Velocity	1 Div. = 0.212 in/sec
	Time	1 Div. = 2 millisec

Fig. 27. Oscilloscope Trace of Displacement-Time and Velocity-Time Curves

diagram, displacement-time curves and velocity-time curves taken from the oscilloscope traces. The form of the phase plot and the curves substantiated that the oscillation was quasi-harmonic. The near circle demonstrated by the phase plot justified the assumption that the mean value from the vibration curves could be utilised for the friction-velocity curves as well as the assumption used in the theoretical analysis that a solution of harmonic nature could be expected.

Attempts were made to work out the zero slope isocline from the phase plane plot obtained from the oscilloscope by reversing the Dudley and Swift [11] graphical method. However, the slight drift in frequency during frictional oscillations requires frequent re-calibration of the oscilloscope. In addition, there is no satisfactory way to establish an accurate tangent to the points on the phase plot. Therefore it was decided not to use these phase plots for analytical purposes.

In the tests performed on sliding surfaces lubricated with 'Petrolatum' oil satisfactory results and consistent oscillations were obtained. This behaviour could be attributed to the uniformity of friction produced by the lubricant film.

Tests were also performed on surfaces coated with resin. Frictional oscillations were observed almost instantly with no run-in distance being required. The amplitude of the oscillations were of large magnitude and increased as the driven surface velocity increased. The oscillation began to die out at a high velocity of approximately 40 in/sec. Fig. 28. shows an amplitude-velocity curve and a

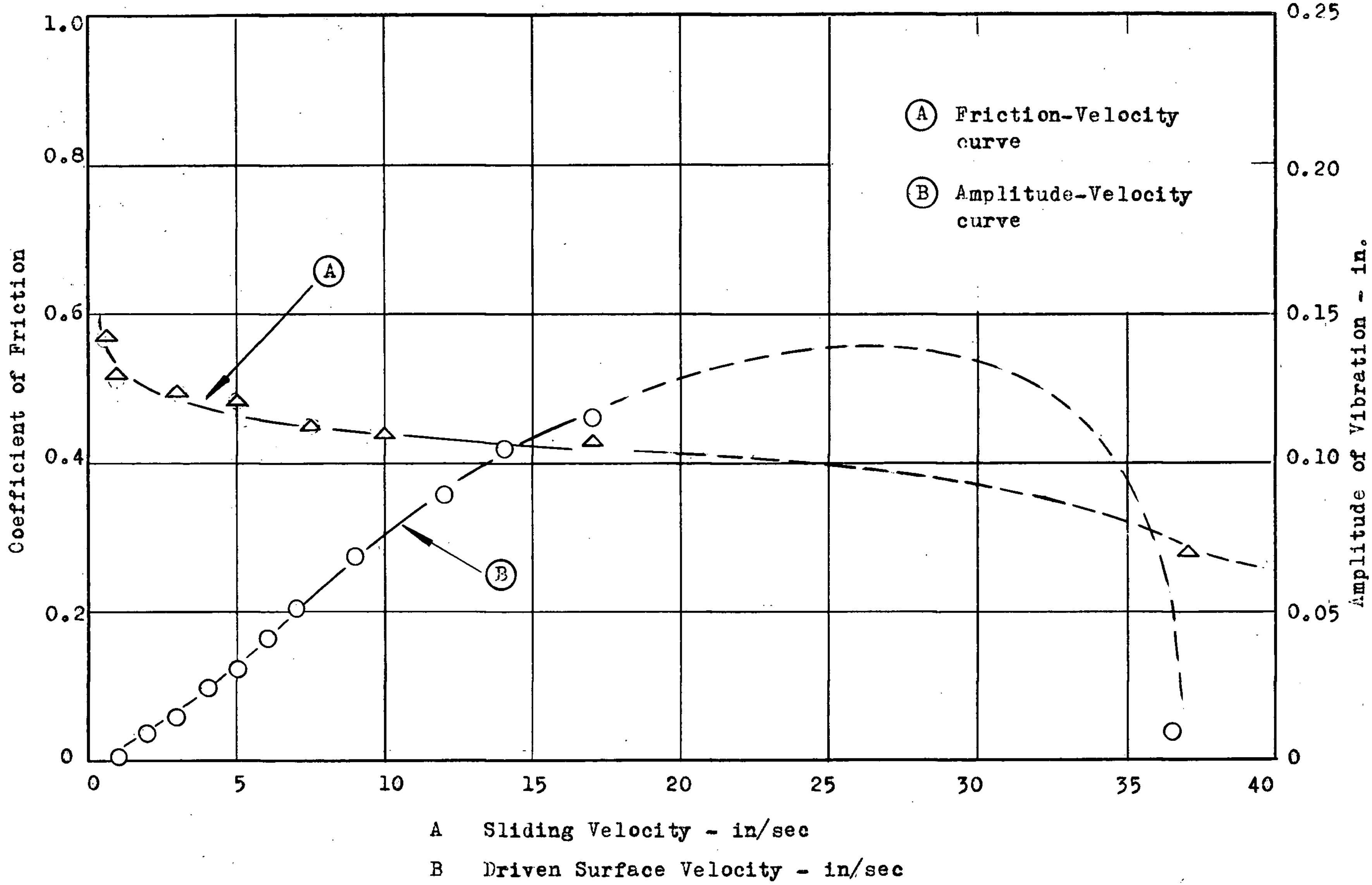

Fig. 28. Graph of Friction-Velocity and Amplitude-Velocity Curves - Resin Coated Surface

friction-velocity curve obtained from resin coated sliding surfaces.

A fine black deposit of wear debris formed on the sliding track was observed during frictional oscillation. Analysis of the debris showed that it consisted of pure iron; iron oxide was not detected.

The effect of the normal load on the amplitude of oscillations was investigated experimentally. The tests were carried out by changing the loads during frictional oscillations. No significant effect was observed.

During each test the frequency of the quasi-harmonic oscillation at various velocities was obtained from the oscillograph trace. The frequency was found to be relatively constant at a value of 19 cps $\pm$ 0.5 cps; the natural frequency of the system as indicated in Appendix C was 19.9 cps.

The experimental curve (C) in Fig. 17 was approximately fitted by a polynomial and was analysed theoretically by the method described earlier. The results were plotted in Fig. 21.

CHAPTER V

DISCUSSION

Stick-Slip and Quasi-Harmonic Oscillations

Dry friction sliding experiments with steel on steel showed that all systems appear to start with an almost flat friction-velocity curve when there is no 'run-in' or when the distance run is less than 150 in., such as the curve (A) shown in Fig. 17. The shape of this curve finds a very close connection with the results obtained by both Potter [17] and Cameron [18]. In their stick-slip investigations, the experimental results show that the static coefficient of friction dropped almost instantly to its kinetic value, and thereafter the kinetic coefficient of friction was found to be constant as the sliding velocity increased. There is no evidence that the surfaces were 'run-in' prior to the tests. In fact, the majority of systems exhibiting stick-slip are slow speed and probably never receive 'run-in' in the true sense. It is therefore quite obvious that throughout each of their tests the total distance run would be well within the run-in distance of curve (A) in Fig. 17. The apparatus used in the present investigation was not designed for low velocity experiments and there was no way of investigating stick-slip phenomena. However, it is believed that stick-slip behaviour would have been observed in the present work prior to run-in if sufficiently low driven surface velocities could have been obtained.

It was found from the present investigation that frictional oscillations of the quasi-harmonic type did not exist until a certain run-in distance had been attained and once vibration appeared, it was found to be stable for disc velocities up to a certain critical value which in turn was observed to be dependent on the shape of the friction-velocity curve. Examination of the surfaces when the oscillation first appeared revealed that a fine black deposit of wear debris had formed on the track. The role of the wear debris in promoting the oscillation is obscure. However, in the experiments performed with resin coated surfaces, frictional oscillations were observed almost instantly and no run-in was required. Considering these findings together suggests that the action of the wear debris might be similar to that of resin on the bow used for playing a stringed instrument.

Combining the work of Potter and Cameron with the present work, a complete picture of the frictional oscillation for dry sliding surfaces with steel on steel has been revealed. On surfaces with little run-in distance, the coefficient of friction has an almost instant drop from its static value to its kinetic value and the friction-velocity characteristic has a linear form. At this stage, only stick-slip type oscillations exist in the system and the amplitude of this form of oscillation decreases as surface velocity increases and eventually disappears at a critical velocity. After a certain run-in distance has been attained, a negative slope region begins to form in the friction-velocity curve. Quasi-harmonic type oscillations then commence at driven surface velocities well above the critical velocity of the stick-slip oscillations. The amplitude of the quasi-harmonic oscillation increases as driven surface velocity increases until a certain velocity is reached whereupon the oscillation becomes unstable and the amplitude drops abruptly.

Comparison of Theoretical and Experimental Results

The theoretical analysis suggested that the amplitude of oscillation would increase as the driven surface velocity increases and the rate of increase would be little affected by the shape of the friction-velocity curves. However the oscillation would become unstable when a certain surface velocity was reached. Further study showed that these unstable oscillations appeared close to the point where the negative region of the friction-velocity curve begins to flatten out. It will be noted from the previous chapter that these findings derived from the theoretical analysis were substantiated by the experimental results. Equation (23) showed that $A = 0$ is always one of the solutions, thus we shall assume that when the oscillation becomes unstable the solution $A = 0$ predominates.

The theoretical analysis also suggested that the frictional oscillations were independent of the relative location of the friction-velocity curve. In other words, the friction-velocity curve as a whole could be shifted up or down along the friction coefficient axis without influencing the amplitude of oscillation.

The effect of the damping coefficient was not investigated experimentally. However, the theoretical analysis suggested that although increasing the damping coefficient had little effect on the amplitude of oscillation it would cause the oscillation to become unstable at an earlier stage. By reference to the graphical construction in Fig. 4. it will be noted that the damping coefficient has the effect of reducing the slope of section AB of curve ABC and at the same time increasing the slope of section BC. Thus increasing the damping coefficient shifts the flattening point of the negative slope of the friction-velocity curve towards the low velocity region. The termination point of the oscillation was found to be closely related to the flattening point of the friction-velocity curve, hence increasing the damping coefficient will cause the oscillation to become unstable at an earlier stage.

One common result observed from the theoretical analysis and from the experiments performed with dry sliding surfaces, resin coated surfaces or lubricated surfaces, was that the amplitude of frictional oscillation increases almost linearly as the driven surface velocity increases, although the termination points of the oscillations were quite different.

Experiments revealed that the run-in effect is highly dependent on the finishing of the sliding surfaces. There is also some evidence that run-in could be affected by surrounding conditions such as temperature and humidity. For the present investigation, no means were used to control these conditions. It is therefore not possible, in the present stage, to predict the exact relationship between the run-in distance and the friction-velocity characteristic. However, the experiments revealed that for the sliding surfaces used in the present work, the curve of coefficient of friction versus distance run has, in general, the shape shown in Fig. 18.

CHAPTER VI

1. Conclusion

A simple approach was adopted for the theoretical analysis in which the frictional coefficient was expressed as a function of sliding velocity only and this was expressed in the form of a polynomial. By using the assumption that a periodic solution would be expected from the non-linear differential equation of the system, the slowly varying amplitude and phase method of Kryloff and Bogoliuboff was used to solve the non-linear equation. A polynomial for the amplitude of oscillation was obtained from the solution. Owing to the complicated calculations involved in finding the polynomial for the friction-velocity curve and consequently solving another polynomial, the problem was solved on the computer. Although the theoretical analysis did not give the exact value of the experimental amplitude-velocity curve, nevertheless it did predict the same trend.

Experiments were carried out on unlubricated surfaces to investigate the behaviour of the quasi-harmonic type frictional oscillations. Strain gauges and a velocity transducer were attached on the vibrating system in order to obtain slider displacement and velocity. Records of the displacement of the slider obtained from the oscillograph trace at different surface velocities were used to investigate the friction-velocity characteristic and the amplitude-velocity relationship. Photographs of the displacement-velocity phase plot obtained from the oscilloscope were used to supplement the oscillograph records for illustrating the type of frictional oscillations.

Experimental results revealed that for short running distances, the friction-velocity curve was almost flat and linear, under these conditions frictional oscillations of the stick-slip type as investigated by Potter [17] and Cameron [18] could occur. As the run-in distance was increased the low velocity region of the friction-velocity curve began to grow. As it grew, the flattening point of the negative slope region shifted towards the high velocity region. Frictional oscillations of the quasi-harmonic type existed in the system when there was a definite growth of the negative slope region of the friction-velocity curve. A black deposit of wear debris observed on the track during frictional oscillation was considered to have an action similar to resin on a stringed instrument. The amplitude of the quasi-harmonic oscillation increased almost linearly as the driven surface velocity was increased until a critical velocity was reached where the friction-velocity curve began to flatten out, beyond this point the oscillation became unstable and eventually died out.

Although no experiments were performed to investigate the damping effect, the theoretical analysis revealed that increasing the degree of damping would lower the value of the critical velocity. The graphical method substantiated this effect.

The motion of the violin string under the action of the bow has been considered as a frictional oscillation phenomena; Lord Rayleigh [26] discusses this motion briefly but offers no detailed explanation of the motion since 'some of the details were still obscure'. The present investigation has connected the behaviour of frictional oscillation of the stick-slip and quasi-harmonic types, thus revealing a more complete picture of the phenomena discussed by Rayleigh.

2. Suggestions for Future Research

The 'run-in' condition has been considered to be affected by the surface condition and the surrounding conditions. Future experimental investigations should be carried out under an atmosphere which would have the humidity and the temperature controlled and, if possible, the surrounding air should be filtered thus eliminating any possibility of particle contamination which, very often, is the cause of surface damage.

The present apparatus should be modified or redesigned so that the curvature effect would be kept to a minimum. Linear movement of the surfaces would be useful but this may not be easily fulfilled when a continuous motion is also required. However the present circular movement could be modified to suit the purpose. This could be done by modifying the self-aligning joint and the cantilever bar so that the slider would bear on the far side of the track instead of the near side, thus permitting the slider to vibrate along a path close to that of the track. The slider and its mount should be redesigned, possibly with a spherically shaped mount.

Future research should relate to a further study of the relationships between the frictional oscillation, the friction-velocity curve and the surface condition. Hence the friction-velocity charateristic could be modified at will in a predetermined manner.

APPENDIX A

Calibration of Oscilloscope

The oscilloscope was used to obtain velocity-displacement phase plane diagrams of the frictional oscillations. In order to obtain a true shape of the phase plane and to determine the scale factors of the axes it was necessary to pre-set the sensitivities of the oscilloscope and the gain control of the Bridge Amplifier Meter. To this end, a sine wave frequency generator (Model hp 200 CD), a Goodmans Vibration Transducer (Model V47) and the Bogen amplifier (Model PDR) were used. The vibration transducer was mounted on one side of the self-aligning joint and was used to vibrate the elastic system. Prior to the calibration, the frequency of the frictional oscillation was noted from the chart record, so that the frequency generator would be set to give the same frequency. The elastic beam was thus excited with a simple harmonic oscillation having the same frequency as the frictional oscillation. A circular phase plane plot is expected for harmonic oscillations, accordingly adjustments were made to the bridge amplifier gain control, the sensitivities of the oscilloscope and the position of the permanent magnet until the best circular phase plane was obtained on the oscilloscope screen. The harmonic oscillation was also recorded in the oscillograph, so that a scale factor for the axes of the phase plane could be determined by comparing the corresponding displacements of the curve on the oscilloscope screen and the oscillograph.

APPENDIX B

Calibration of the Vibration Apparatus

Calibration of the vibration apparatus had been carried out earlier by Pomeroy [25] but several slight modifications to the apparatus dictated recalibration.

1. Calibration of Load System

The calibration followed the same procedure as carried out by Pomeroy. A strain ring was used in conjunction with the Brush Universal Analyser. From the calibration curves, it was determined that for each pound on the load pan an equivalent of 0.492 lb acted normally at the slider.

2. Calibration of Frictional Force and Strain Gauges

A pulley system was set up on one side of the self-aligning joint. One end of a smooth cord was fastened to the joint and the other end was passed round the pulley and attached to a load pan. Deflections of the elastic beam due to weights added to the load pan were recorded on the oscillograph. Deflection-load curves were plotted and a straight line was drawn. The slope of the force at slider versus pen deflection curves was found to be 0.234 lb/mm. Next a depth micrometer was rigidly mounted with its spindle lying horizontally and imposed perpendicular to the side of the self-aligning joint. The beam was then gradually deflected by the micrometer. Results obtained from the oscillograph were plotted against the true displacement of the self-aligning joint. A straight line was drawn and the slope of slider displacement against pen deflection was found to be 0.00332 in/mm. Hence the stiffness of the elastic system was 70.5 lb/in.

The calibration of the Brush Universal Analyser followed the procedure as given in the maker's manual. The gain control was adjusted to give the oscillograph 15 mm pen deflection when the attenuation factor of the Universal Analyser was set at 5.

APPENDIX C

Determination of the System Damping Coefficient

The elastic beam was given an initial displacement and then released in free vibration. Chart records of the free vibrations were obtained from the oscillograph. Five tests were carried out. For each test the amplitudes of vibration of every tenth cycle were recorded and the ratio between consecutive amplitudes was calculated. The average amplitude ratio and the frequency from the five tests were used for determining the damping coefficient.

The logarithm of the vibration amplitudes were plotted against the cycle numbers. The curve was found to be linear thus suggesting that the damping coefficient of the system was proportional to the velocity of vibration,

The average amplitude ratio $\dfrac{X_n}{X_{n+10}} = 1.225$

Frequency of free vibration $\omega_d = 19.9$ cps

Now $\dfrac{X_n}{X_{n+10}} = e^{20\pi \frac{\Delta}{\omega_d}}$ where $\Delta = \dfrac{r}{2M}$

The equation of motion is

$$M\ddot{X} + r\dot{X} + kX = 0$$

$$\log_e 1.225 = 20\pi \frac{\Delta}{\omega_d}$$

$$\Delta = 0.404 \text{ rad./sec}$$

The natural frequency $\omega = \sqrt{k/M} = \sqrt{\omega_d^2 + \Delta^2}$

$\therefore\ \omega = 19.9 \times 2\pi \text{rad./sec}$

The equivalent mass of the system was $M = 1.76$ lb

and the damping coefficient of the system $r = 0.00368$ lb.in/sec

Surface Profile of Specimens

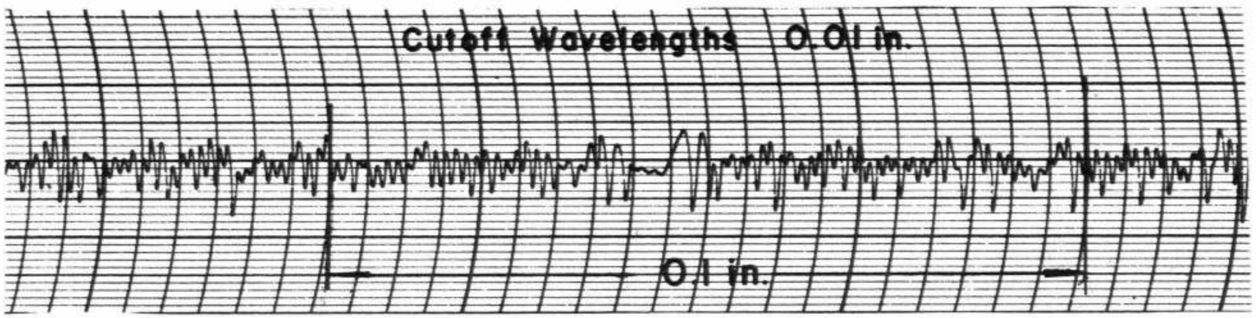

Surface Profile Before Test 7.5 Microinches RMS

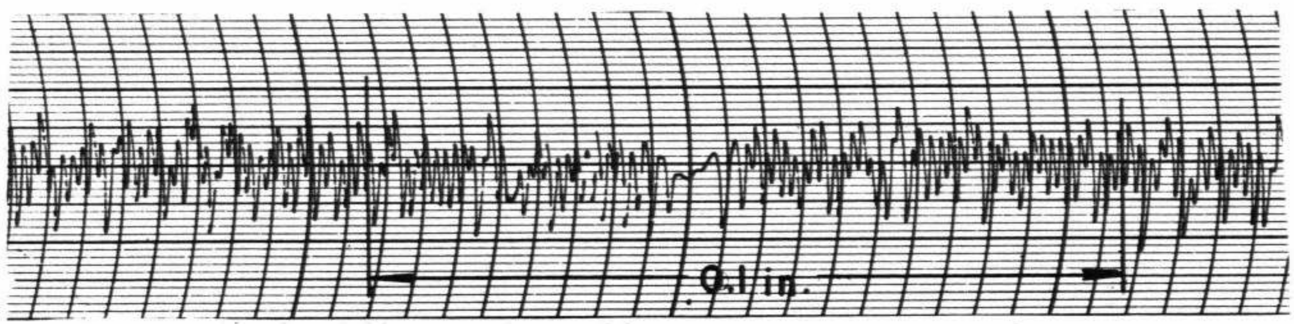

Surface Profile After Test 15 Microinches RMS

Lathe Machining and Polishing with Emery Paper

Fig. 29. Oscillograph Trace of Surface Profile

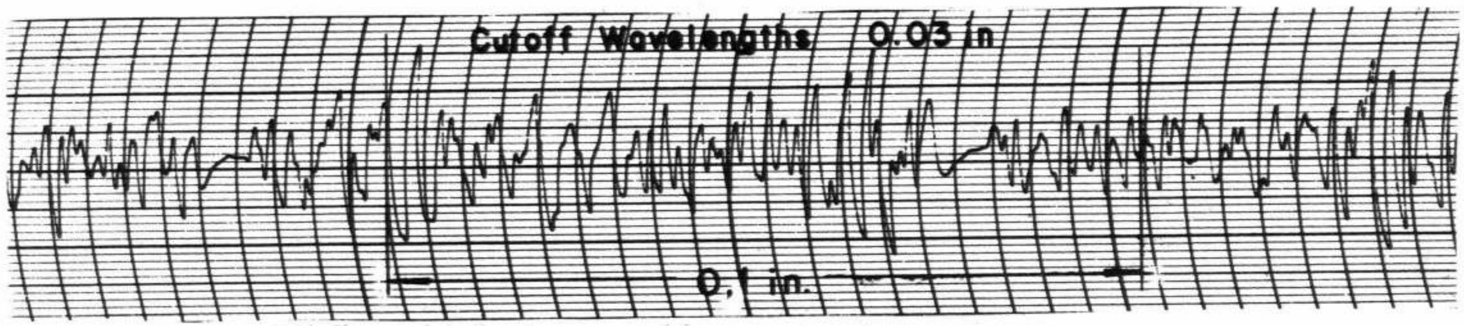

Surface Profile Before Test 39 microinches RMS

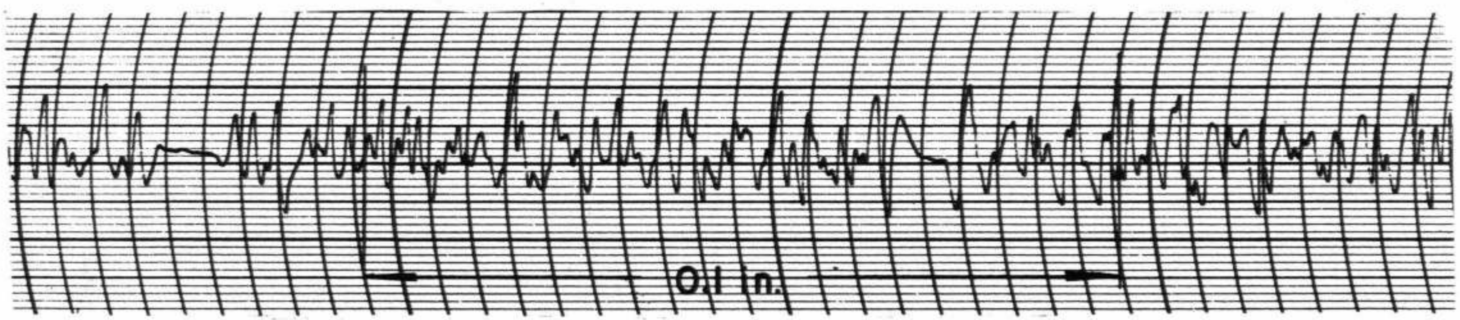

Surface Profile After Test 31 microinches RMS

Grinding and Lapping with Carborundum

Fig. 30. Oscillograph Trace of Surface Profile

BIBLIOGRAPHY

1 Froude, W. referred to by McLachlan, N.W. "Ordinary Non-Linear Differential Equations in Engineering and Physical Sciences", Oxford University Press.

2 Thomas, S. "Vibrations Damped by Solid Friction", The Philosophical Magazine, Series 7, Vol. 9, p. 329, 1930.

3 Papenhuyzen, P.J. "Wrijvings Proeven in Verbandmet het Slippen Van Autobanden", De Ingenieur, 53, p. 75, 1938.

4 Bowden, F.P. and Leben, L. "The Nature of Sliding and The Analysis of Friction", Proceeding of the Royal Society, A 169, p. 371, 1939.

5 Blok, H. "Fundamental Aspects of Boundary Lubrication", Journal of Soc. of Automotive Engineers, Vol. 46, p. 54, Feb. 1940.

6 Morgan, F., Muskat, M., and Reed, D.W. "Friction Phenomena and the Stick-Slip Process" Journal of Applied Physics, Vol. 12, p. 743, Oct. 1941.

7 Sampson, J.B., Morgan, F., Muskat, M., and Reed, D.W. "Friction Behaviour during the Slip Portion of the Stick-Slip Process", Journal of Applied Physics, Vol. 14, p. 689, Dec. 1943.

8 Rabinowicz, E. "The Nature of the Static and Kinetic Coefficient of Friction", Journal of Applied Physics, Vol. 22, p. 1373, Nov. 1951.

9 Bristow, J.R. "Kinetic Boundary Friction", Proceeding of the Royal Society, Vol. 189, p. 88, 1945.

10 Bristow, J.R. "The Measurement of Kinetic Boundary Friction, or The Experimental Investigation of 'Oiliness'", Proceedings of the Institution of Mechanical Engineers, Vol. 160, p. 259, 1949.

11 Dudley, B.R. and Swift, H.W. "Frictional Relaxation Oscillations", The Philosophical Magazine, Series 7, Vol. 40, p. 849, 1949.

12 Sinclair, D. "Frictional Vibrations", Journal of Applied Mechanics, p. 207, June, 1955.

13 Rabinowicz, E. "A Study of Stick-Slip Process", Proceedings of The Symposium on Friction and Wear, Detroit, 1957.

14 Derjaguin, B.V., Push, V.E., and Tolstoi, D.M. "A Theory of Stick-Slip Slidings of Solids", Proceedings of The Conference on Lubrication and Wear, p. 257, Oct. 1957.

15 Singh, B.R. "A Study of Critical Velocity of Stick-Slip Sliding" Trans. ASME, Journal of Engineering for Industry, p. 393, Nov. 1960.

16 Cook, N.H. "A Study of Dynamic Friction", ASME Paper 58-A-257, 1958.

17 Potter, A.F. "A Study of Friction Induced Vibrations", M.A.Sc. Thesis in Mechanical Engineering, The University of British Columbia, 1963.

18 Cameron, R. "Friction Induced Vibration", M.A.Sc. Thesis in Mechanical Engineering, The University of British Columbia, 1963.

19 Brockley, C.A., Cameron, R., and Potter, A.F. "Friction Induced Vibration". In press, ASME, 1965.

20 Jarvis, R.P. and Mills, B. "Vibrations Induced by Dry Friction", Proceedings of the Institution of Mechanical Engineers, Vol. 178, Part 1, Number 32, 1963.

21 Kosterin, J.I. and Kraghelsky, I.V. "Relaxation Oscillations in Elastic Friction Systems", Friction and Wear in Machinery, ASME. A translation of TPEHNE N N3HOC B MAIIINHAX, Vol. 12, 1958.

22 Kosterin, J.I. and Kraghelsky, I.V. "Rheological Phenomena in Dry Friction", Institute of Machine Study, Academy of Sciences of the USSR.

23 Kryloff, N. and Bogoliuboff, N. "Introduction to Non-Linear Mechanics", (Translated from Russian by Lefschetz, S.) Oxford University Press, London, and Princeton University Press, N.J., U.S.A.

24 Sohon, H. "Engineering Mathematics", D. Van Nostrand Co.

25 Pomeroy, R.J. "Frictional Transition Effects in Unlubricated Sliding", M.A.Sc. Thesis in Mechanical Engineering, The University of British Columbia, 1963.

26 Lord Rayleigh, "Theory of Sound", Dover Publications, 1945, Vol. 1, p. 208.